Passive Tension in Cardiac Muscle: Contribution of Collagen, Titin, Microtubules, and Intermediate Filaments

Henk L. Granzier and Thomas C. Irving
Department of Veterinary and Comparative Anatomy, Pharmacology, and Physiology, Washington State University, Pullman, Washington 99164-6520 USA

ABSTRACT The passive tension-sarcomere length relation of rat cardiac muscle was investigated by studying passive (or not activated) single myocytes and trabeculae. The contribution of collagen, titin, microtubules, and intermediate filaments to tension and stiffness was investigated by measuring (1) the effects of KCl/KI extraction on both trabeculae and single myocytes, (2) the effect of trypsin digestion on single myocytes, and (3) the effect of colchicine on single myocytes. It was found that over the working range of sarcomeres in the heart (lengths ~1.9–2.2 μm), collagen and titin are the most important contributors to passive tension with titin dominating at the shorter end of the working range and collagen at longer lengths. Microtubules made a modest contribution to passive tension in some cells, but on average their contribution was not significant. Finally, intermediate filaments contributed about 10% to passive tension of trabeculae at sarcomere lengths from ~1.9 to 2.1 μm, and their contribution dropped to only a few percent at longer lengths. At physiological sarcomere lengths of the heart, cardiac titin developed much higher tensions (>20-fold) than did skeletal muscle titin at comparable lengths. This might be related to the finding that cardiac titin has a molecular mass of 2.5 MDa, 0.3–0.5 MDa smaller than titin of mammalian skeletal muscle, which is predicted to result in a much shorter extensible titin segment in the I-band of cardiac muscle. Passive stress plotted versus the strain of the extensible titin segment showed that the stress-strain relationships are similar in cardiac and skeletal muscle. The difference in passive stress between cardiac and skeletal muscle at the sarcomere level predominantly resulted from much higher strains of the I-segment of cardiac titin at a given sarcomere length. By expressing a smaller titin isoform, without changing the properties of the molecule itself, cardiac muscle is able to develop significant levels of passive tension at physiological sarcomere lengths.

INTRODUCTION

When passive muscle is stretched beyond its slack length, it develops passive tension. In comparison with active tension, which is based on actomyosin interaction, relatively little attention has been focused on the source of this passive tension. This situation is rapidly changing, however, because of the discovery of the endo-sarcomeric elastic protein titin (also known as connectin), which in striated muscle spans from the Z-line to the M-line of the sarcomere and that may provide a molecular basis for passive tension (for reviews, see Wang, 1985; Maruyama, 1986; Trinick, 1991). The segment of the titin molecule that is found in the I-band behaves as an elastic connector that connects the A-band to the Z-line and is presumed to develop passive tension when sarcomeres are stretched (Wang et al., 1984; Furst et al., 1988). This notion is supported by recent studies on skeletal muscle fibers that express size variants of titin and that have elastic titin I-segments that have different lengths when unstrained (Wang et al., 1991; Granzier and Wang, 1993a, b). The passive tension-sarcomere strain curves of these fibers are very different, whereas the passive tension-I-segment strain curves are virtually indistinguishable (Wang et al., 1991; Granzier and Wang, 1993b), suggesting that the strain of the I-segment of titin determines how much passive tension a skeletal muscle fiber develops.

Passive tension is an important factor in cardiac muscle because it is part of the diastolic wall tension that determines the extent of filling of the heart and its subsequent stroke volume (for reviews, see Allen and Kentish, 1985; Brady, 1991a). Passive tension is also important in the activated myocardium because it has been shown that it is one of the factors that determines the shortening velocity of trabeculae (De Tombe and ter Keurs, 1992) and cardiac myocytes (Sweitzer and Moss, 1993). It is difficult to predict a priori the importance of titin to passive tension of the heart. In addition to titin, cardiac muscle contains a well developed cytoskeleton with a high concentration of desmin-based intermediate filaments (Tokuyasu, 1983; Price, 1984) that also may develop passive tension (Wang et al., 1993). Furthermore, the myocardium contains a dense collagen network that is likely to function as an extracellular source of passive tension (for review, see Weber et al., 1994). The present study was conducted to determine the contribution of titin to passive tension of the heart, relative to that of the extracellular matrix (collagen) and other intracellular cytoskeletal elements (microtubules and intermediate filaments).

We studied the passive properties of single myocytes obtained by collagenase digestion of the rat heart and developed cell isolation and skinning protocols that kept titin intact. (This protein is notoriously sensitive to proteolysis; e.g., Granzier and Wang, 1993c). The gluing method used by Sweitzer and Moss (1993) to study active tension in rat myocytes was adapted and used to study passive tension.

Received for publication 12 September 1994 and in final form 16 November 1994.

Address reprint requests to Dr. Henk L. Granzier, Dept. of VCAPP, Washington State University, 205 Wegner Hall, Pullman, WA 99164-6520. E-mail: granzier@unicorn.it.wsu.edu.

Dr. Irving's current address: Division of Biology, Illinois Institute of Technology, 3101 South Dearborn Street, Chicago, IL 60616.

0006-3495/95/03/1027/18 $2.00

Sarcomere length was monitored using digital image processing of videotaped images of myocytes during the mechanical protocols. The contribution of collagen was studied by comparing the mechanical properties of the myocytes with those measured on trabeculae, using identical mechanical stretch/release protocols.

We found that over the working range of sarcomeres in the heart (lengths ~1.9–2.2 μm), titin and collagen are the main contributors to passive tension, with titin predominating at shorter lengths and collagen predominating at longer lengths. It was also found that at physiological sarcomere lengths of the heart, cardiac titin develops much higher tensions than does skeletal muscle titin at similar sarcomere lengths, and we show that this results predominantly from much higher strains of the I-segment of cardiac titin and not from differences in the stress-strain characteristics of cardiac titin. At physiological sarcomere lengths, intermediate filaments contribute ~10% to passive tension, whereas microtubules contribute to passive tension in some cells, but on average their contribution is not significant.

MATERIALS AND METHODS

Preparations

Cardiac myocytes

Single myocytes were isolated (cf. Bihler et al., 1983) using collagenase digestion of the adult rat heart (male Sprague Dawley, 225–250 g, 8–10 weeks). The coronary arteries were perfused with an oxygenated Krebs solution (NaCl: 127 mM; KCl: 7.4 mM; $NaHCO_3$: 21 mM; $MgCl_2$: 1 mM; NaH_2PO_4: 0.3 mM; dextrose: 11 mM; insulin: 2.5 IU/l; pH: 7.4, 37°C) at 6.5 ml/min and 37°C for: (1) 5 min with no added Ca^{2+}; (2) 25 min with 75 μM Ca^{2+}, 0.5 mg/ml collagenase (Worthington, Type II), and 0.3 mg/ml hyaluronidase (Sigma, type 1-S); (3) 20 min with 15 mM 2,3-butane-dione monoxime. The atria were then removed, and the left and right ventricles were separated; the septum was assumed to be part of the left ventricle. The ventricles were cut into small pieces that were gently drawn several times through plastic pipettes. This released large numbers of isolated cells of which the majority were rod-like. Because we also obtained small groups of cells that were still attached to each other, we decided to increase the likelihood that collagen was completely removed from the isolated cells by treating the cells once again with collagenase as described above. Cells were subsequently washed by letting them settle in test tubes, removing the supernatant and gently resuspending the cells (volume ~0.5 ml) in 14 ml of fresh medium containing 0.04 mM leupeptin and 0.5 mM PMSF. Washing was repeated 8 times. This procedure diluted collagenase and hyaluronidase and their contaminants by more than a factor of 10^{11}. If this washing was omitted, then titin was often degraded after skinning of the cells. A high yield of cells was obtained ($2.3 \pm 0.3 \times 10^6$ cells/heart) of which $54 \pm 3\%$ ($n = 16$) were elongated and rod-like. Before skinning the majority of the rod-like cells were calcium-tolerant, whereas after skinning cells responded to calcium with a vigorous contraction.

Cells were skinned in relaxing solution (imidazole: 40 mm; EGTA: 10 mM; MgAc: 6.4 mM; NaATP: 5.9 mM; NaN_3: 5 mM; K-proprionate: 80 mM; creatine-phosphate: 10 mM; DTT: 1 mM; pH 7.0, 20°C; leupeptin: 0.04 mM; PMSF 0.5 mM). For most experiments, 0.25% (w/v) purified Triton X-100 (28314; Pierce Chemical Co.) was used for 50 min. Cells were then washed 2 times with relaxing solution (as above) and stored for at least 3 h at 0°C until they were used. For experiments on microtubules, cells were skinned at room temperature with staphylococcal α-toxins (GibcoBRL) at 250 units/ml. Cells were skinned for 60 min because preliminary studies showed that this was the minimal duration that allowed us to reversibly put cells in rigor.

Trabeculae

Right ventricle trabeculae were dissected from the adult rat heart (male Sprague Dawley, 250–300 g, 11–14 weeks) in oxygenated Krebs solution (NaCl: 118 mM; KCl: 5 mM; $NaHCO_3$: 20 mM; $MgSO_4$: 1.2 mM; NaH_2PO_4: 1.7 mM; BDM: 15 mM; Dextrose: 11 mM; insulin: 2.5 IU/l; pH: 7.2, 5°C). The preparations were dissected free from their attachment to the heart and then skinned in relaxing solution (see above) with 1% Triton X-100 for 1 h. The trabeculae were subsequently washed with relaxing solution and stored for 3 h at 0–4°C before they were used.

Mechanics

Myocytes

The mechanical set-up was built around an inverted microscope (Nikon Diaphot TMD) that was equipped for phase-contrast and epifluorescence microscopy, and that was placed on top of a vibration isolation table (Micro-G, model 63–573, Technical Manufacturing Corp.). Cells were attached at one end to a motor (model 6800, Cambridge Technology Inc.; step response 0.5 ms; RMS position noise: ~0.5 μm) and at the other end to a high resolution force transducer (model 406A, Cambridge Technology; bandwidth DC-90 Hz) that was calibrated with weights of known mass. The peak-to-peak noise of the force transducer without a cell attached is ~1 μg. However, with an attached myocyte and during slow ramp stretches, peak-to-peak force noise is typically 10–20 μg. The force transducer and motor were mounted to manipulators attached to the XY stage of the microscope. Mounted to the stage was also a hydraulic XYZ manipulator (NRC MX630) with a glass micro-needle attached at the end that protruded into the chamber, and that was used to manipulate cells. The flow-through chamber in which the cells were placed had a glass coverslip as bottom. Before cells were added to the chamber, the chamber was coated with BSA at 0.5 mg/ml in relaxing solution to prevent cells from sticking to the glass. The chamber had a volume of about 100 μl, contained a small J-type thermocouple, and could be temperature-controlled (0–40°C). The temperature in all experiments reported here was controlled at 20°C.

For cell attachment to the transducers, we used the tip of minutien pins (Fine Science Tools). At their blunt end, the pins were attached to the transducers, using paraffin. Their pointed end (diameter ~10–20 μm) was immersed in the chamber and glued to cells. To maximize the cell attachment area, the tip of the needle was bent such that it was perpendicular to the long axis of the cell. After testing many different types of glue, we concluded that the best cell attachment could be achieved following the method of Sweitzer and Moss (1993), which uses "Great Stuff" (Insta-Foam Products, Inc.).

Using the glass micro-needle, we first aligned the cell such that it was perpendicular to the hooks. We then placed one of the hooks above part of the cell where we intended to make the attachment. The hook was then raised out of the solution, and with the aid of a high-power stereo-microscope, a small amount of glue was applied to the end of the hook (it is critical to have the optimal amount of glue). The hook was then quickly lowered into the chamber and gently pushed on top of the cell, after which the hook was raised and the cell was elevated from the bottom. Before gluing the other end of the cell, we used the glass micro-needle to push the free end of the cell upward so that the cross section of the cell could be viewed (Fig. 1 *B*), to determine its area. Next the other end of the cell was glued. Before stretching the cell, ample time (>45 min) was allowed for the glue to set. The obtained cell attachments were able to withstand forces as high as 3–5 mg, and even when cells were stretched to the point of breakage, cells did typically not completely detach from the hooks.

Trabeculae

The same mechanical setup was used as described above, including the same motor. The force transducer, however, was now a strain-gauge (AME 801E, Horton, Norway) with a strain gauge conditioning amplifier (model 2310, Measurement Group, Inc.) used at a bandwidth of DC-1000 Hz. Peak-to-peak force noise measured when trabeculae were slowly stretched was

typically 100–200 μg. To mount trabeculae in the setup, a small T-shaped aluminum clip was glued to each end of the preparation as explained in Granzier and Wang (1993a).

Sarcomere length measurement

Myocytes

Cells were imaged with a 40 × phase-contrast objective (Nikon ELWD Plan40/0.55 NA) and a long working distance phase-contrast condenser (Nikon LWD 0.52), equipped with phase-3 optics. The depth of focus of these optics (Slayter and Slayter, 1992) is about 1 μm. Images of the cell were collected through the video port of the microscope, using a Watek model 902 CCD camera (Edmund Scientific). The video signal was sent through a real-time image processor (Argus-10, Hamamatsu), for contrast enhancement and the addition of a timer signal (accurate to 1 ms) and was then stored on VHS video tape. Care was taken that the long axis of the cell was aligned with the long axis of the video image. Optical magnification was calibrated using diffraction gratings.

Videotaped records were digitized into 8-bit, gray-scale images using the built-in frame grabber of a Macintosh Quadra 840AV microcomputer and saved as a QuickTime MooV using the program FusionRecorder (Video-Fusion Inc., as supplied with the 840AV). An example of an individual digitized frame is shown in Fig. 1 *A*. To keep the amount of data manageable, the video sequence was digitized at 0.075–0.2 frames per second (fps) depending on the duration of the stretch protocols (some lasting >2000 s) although up to 4 fps was possible with this set-up. Digitized images were then analyzed using ImageQuickTime, a version of the public domain program National Institutes of Health Image (v1.51, originally written by W. Rasband at the National Institutes of Health, adapted by E. Shelden, University of Connecticut to read QuickTime MooV's. National Institutes of Health Image and Image QuickTime available by anonymous FTP from zippy.nimh.nih.gov). The user then defined a region of interest (ROI) in the cell, typically 200 × 16 pixels in size, or about 50 μm × 4 μm. Custom routines written in National Institutes of Health Image macro language were used to save a column-averaged density trace along the long axis of the ROI for each digitized frame. During length change of the cell, both translation and the increase in length of sarcomeres within the original ROI were compensated by varying the size (length and width) and the two-dimensional position of the ROI in the cell such that the same sarcomeres were being sampled throughout the protocol. Density traces were saved in individual files as one trace per digitized frame. Fig. 1 *C* shows examples of ROIs and densitometry traces at short and long sarcomere lengths (*top* and *bottom* trace, respectively).

Density traces were analyzed using custom-written FORTRAN routines to determine the average sarcomere length. Traces were rescaled so that their average value was zero and then embedded into a 2048-element array of zeros. These arrays were discrete fourier-transformed and used to calculate the power spectrum for each frame.

The position of the main peak in the power spectrum was used to calculate sarcomere length. During the course of this work, it was found to be very helpful to plot the evolution of the power spectra with time as three-dimensional plots (e.g., Fig. 1 *D*) to identify clearly the peak after the stretch. Peak position in a given frame was identified by the experimenter, and the program then located the peak position in the following frames using a window centered around the peak position in the previous frame. The behavior of sarcomeres could thus be followed, and artifacts caused by anomalous densities due to mitochondria, for example, in a particular series of frames could be reduced. The width of the power peak at half maximum was used as a measure of the width of the sarcomere length distribution within the sampled area of the cell. The measurements were deconvoluted with the fourier transform of the width of the ROI to give a true distribution. For each frame, we saved into a file the calculated sarcomere length, the width of the sarcomere length distribution, and the proportion of total power. This file could be plotted using a standard commercial plotting package giving, for example, a plot of sarcomere length versus time (Fig. 1 *E*). Tests revealed that the sarcomere length resolution was ~40 nm.

To gain insight into the sarcomere length variation over the width of the cell, we typically analyzed 3–4 ROIs that were each 4 μm wide. Ideally, we would like to analyze the whole cell image, but because it was necessary to exclude parts of the image that contained nuclei and other anomalies, our combined ROIs typically encompassed 50–75% of the cell width. This analysis revealed that the sarcomere length varied somewhat across the cell, especially at the extreme sarcomere lengths that were reached in some of the protocols (Fig. 1 *F*). We analyzed a total of 53 ROIs in 10 cells, and at an average sarcomere length of 3.25 μm, their SD was 0.4 μm, with the shortest sarcomere length at 2.2 μm and the longest at 4.25 μm.

To obtain the average behavior of the different ROIs, we fitted the individual sarcomere length-time relationships with a linear function and then averaged the curves for the different regions. This average sarcomere length-time relationship for a particular stretch-release experiment together with its tension-time and stiffness-time relations (see below) were then used to obtain the force-sarcomere length and stiffness-sarcomere length relations that are presented in Results.

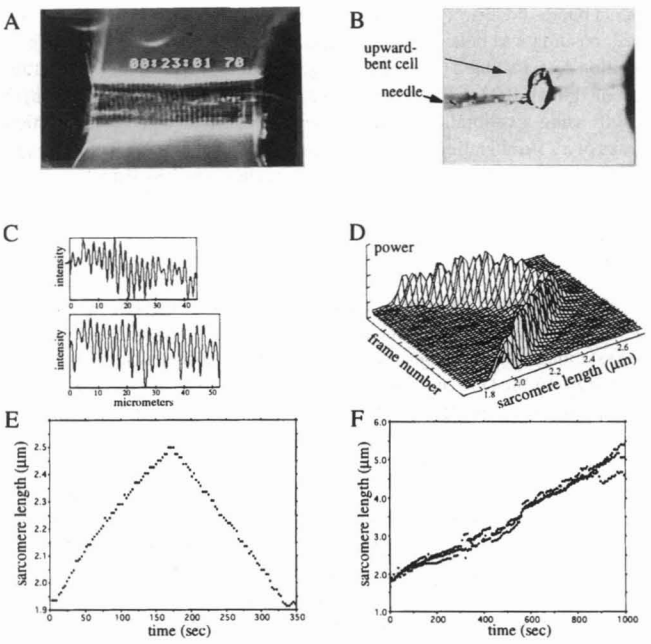

FIGURE 1 Sarcomere length measurement in cardiac cells. (*A*) Image of a cell glued at one end to a small hook attached to a force transducer and at the other end to a hook connected to a motor, for change in cell length and measurement of force. (*B*) Cell glued at only one end while the free end is bent upwards allowing the cross section of the cell to be viewed and its area to be determined. (*C*) Densitometry of a region of interest (ROI) about 24 sarcomeres long and 4 myofibrils wide. The fluctuating density is caused by the striations. The top shows the ROI while the cell is short and the bottom after stretch. Note that to capture the same sarcomeres after stretch, the length of the ROI was increased (in addition to altering the two-dimensional position of the ROI in the cell). (*D*) Power spectrum obtained by discrete fourier transforming the density slices of the ROI during a protocol in which the cell was elongated with a constant velocity and then released with the same velocity. (*E*) Sarcomere length-time relation of a ROI in a cell that was stretched and then released. (*F*) Superimposed sarcomere traces of three different ROIs from the same cell during a stretch from 1.8 to ~5.0 μm. The three ROIs show minor differences in sarcomere behavior, especially at the extreme degrees of stretch. See text for further details.

Trabeculae

Sarcomere length was measured with laser-diffraction using a He-Ne laser beam focused to a diameter of about 250 μm. The diffraction pattern was collected with a bright-field objective (Nikon, ELWD plan 40/0.55); a telescope lens was focused on the back focal plane of the objective, and the diffraction pattern was projected, after compression with a cylindrical lens,

onto a photo-diode array (Reticon RL 256 C/17). The first-order diffraction peak position was obtained (cf. Granzier et al. (1987), using a digital spot-position detector board (Bioengineering, University of Washington, Seattle) installed in an IBM AT computer. This signal was converted to sarcomere length using a calibration curve that was established with the diffraction peaks of a 25 μm grating that was present in the chamber. Sarcomere length noise (peak-to-peak) during slow ramp stretches was less than 10 nm.

Protocols

To obtain reproducible results, myocytes and trabeculae were subjected to stretch and release cycles generated by a computer-controlled mechanics workstation that was designed to impose identical mechanical protocols. It contained 16-bit D/A and 16-bit A/D converters that allowed very slow stretch rates to be imposed on the preparations and small amplitude signals to be sampled. All protocols were generated using an IBM AT (486 processor) computer and a D/A board (DT 2823; Data-translation Inc.) with 100-kHz throughput. Force, cell/fiber length, and sarcomere length were recorded using another acquisition board (DT 2823). The software for the protocols and for data acquisition was written using Asyst (Version 3.0; Asyst Software Technologies).

The cells/trabeculae were stretched with a constant velocity to a predetermined amplitude and then released to the initial length. At least 15 min of rest was allowed before another stretch/release cycle was imposed. Cell length, sarcomere length, and tension were measured every 350 ms. Concurrently, dynamic stiffness was also measured using sinusoidal length perturbations, to allow us to compare results of our study with those of earlier studies on myocytes in which only stiffness was measured (for review, see Brady, 1991a). Every 350 ms the preparation was subjected to a brief, 57-ms burst of sinusoidal length oscillations (70 Hz; amplitude 1% of cell length). Each burst consisted of four oscillations (generated digitally). The ensuing tension oscillations were sampled, and the tension amplitude determined, on-line, using FFT analysis. Stiffness was calculated as the ratio of the tension amplitude to strain amplitude, and the time course of stiffness was plotted.

In earlier work, protocols were used in which stretches and releases were interrupted periodically by long rest periods during which length was kept constant to allow stress relaxation to occur (Granzier and Wang, 1993a). However, in subsequent studies (Granzier and Wang, 1993b) such periods of stress relaxation were omitted because stress relaxation is a continuous process and a steady stress is not attained no matter the duration of the resting period (White, 1983; H. L. Granzier, unpublished observations). An important advantage of the new protocol is that it is completed about 10-fold faster than the previously used protocols in which rest periods were imposed, reducing long term drift in the force signals and allowing more extensive experiments to be carried out on the same cell.

The stretches used for the myocyte work were similar to those used on various other muscle types in previous studies (Granzier and Wang, 1993a, b). In those studies, we found that for comparing the passive tension-sarcomere length relations of different preparations, it is best to use stretch rates that result in a similar I-band stretch rate. In the present study, we therefore used the same I-band stretch rate as of the previous studies on other muscle types: 150%/90 s. In cardiac cells where the I-band is about 0.3 μm (Table 2), this rate corresponds to a sarcomere stretch velocity of 0.005 μm/s.

In those experiments in which we followed the time course of changes in passive tension and passive stiffness (e.g., during trypsin treatment) the stretch/release protocol was altered (see below) so that it could be repeated more frequently, allowing a more detailed study of this time course.

A-band width measurement

We measured the width of the A-band in cardiac cells with a Nikon Diaphot 300 microscope containing a 100×/1.3 NA phase-contrast objective and a 1.25 NA phase condenser. Images were sent through an image processor (Argus-10, Hamamatsu) and then stored on S-VHS video tape. Sequences of 10–15 frames were digitized with the Macintosh Quadra 840AV computer (see above) and averaged to form a single image. For each experimental condition, A-band measurements were made on four different cells. Density profiles for 3–4 regions per cell each containing 4–8 individual A-band profiles were generated. Only regions of the cell that showed clear Z-lines, allowing us to identify positively the A-band, were chosen for the density slices. The A-band width was estimated as the full width at half-maximum (FWHM) of the A-band profiles (cf. Huxley and Niedergerke, 1958). About 100 individual A-band measurements were averaged for each experimental condition.

Gel electrophoresis and gel staining

To determine the molecular mass of titin from the rat heart, we quick-froze whole hearts in liquid nitrogen, pulverized the tissue to a fine powder using a mortar and pestle bathed in liquid nitrogen, and then rapidly added one volume of cold powder to 9 volumes of hot 1.1× solubilization buffer (50 mM Tris-Cl, 2% SDS, 10% glycerol, 80 mM DTT, 30 μg/ml Pyronin Y, pH 6.8 at 25°C) in a homogenizer, present in a water bath of 90–95°C. The sample was solubilized for 90 s and then cooled down and analyzed with SDS-PAGE. For comparison, we also solubilized psoas and semitendinosus muscle from the rabbit using the same procedure as described for the heart. The protein composition of myocytes and trabeculae was determined following the method explained in Granzier and Wang (1993c). Gels were either stained with Coomassie blue or stained for 3.5 min using a ammoniacal silver-stain as detailed in Granzier and Wang (1993c).

Quantitative analysis of electrophoretic gels

Wet gels were scanned at 400 dpi using a UMAX model UC1260 flatbed scanner. Green filters (#60, 403, Edmund Scientific Co.) were used to narrow the bandwidth of the excitation light to that of the absorption spectrum of Coomassie blue and to compensate for the low density cutoff of this scanner. Scanned images were analyzed using National Institutes of Health Image (v 1.55, W. Rasband, NIMH, National Institutes of Health) using the macros supplied with that program. Images were calibrated using a 10-step (0.1–1.0 OD) density filter (#32599, Edmund Scientific Co.) scanned simultaneously with the gel. Only bands whose intensities fell within that of the stepped density filter were analyzed. The various titin peaks often overlapped, and to determine their individual areas, band-averaged density profiles of the calibrated image were saved as text files and imported into Kaleidagraph (Synergy Software). Frequently, there were two major titin peaks, and their areas were determined by fitting them with a two-Gaussian model using the nonlinear least-squares algorithm built into Kaleidagraph. Minor peaks that were sometimes present were estimated by subtracting off the major peaks and then determining the remaining peak areas by numerical integration. Although no systematic attempt was made to estimate errors in the fits, the variation of results in repeated fits was in the 10–20% range.

Because the total amount of protein that was loaded on the gels could not be controlled accurately, we normalized the amount of titin in control cells relative to that of myosin, and in KCl-extracted and trypsin-treated cells relative to that of actin. Normalization had only a minor effect on the results.

Trypsin treatment

Mild trypsin digestion has been used successfully on skeletal muscle to specifically degrade titin and study its involvement in passive tension development (Yoshioka et al., 1986; Funatsu et al., 1990; Higuchi, 1992), and we carried out similar experiments on cardiac cells. Leupeptin was first removed from the skinned cells by letting the cells settle in test tubes, removing the supernatant and gently resuspending the cells (volume ~0.5 ml) in 13 ml of leupeptin-free relaxing solution. This washing procedure was repeated 5 times, which diluted leupeptin by a factor of more than 10^5. Trypsin (Sigma, type III, 12, 700 BAEE units/mg) was made up fresh in leupeptin-free relaxing solution at a concentration of 0.5 μg/ml. We carefully standardized the trypsin preparation and used it a fixed time (30 min) after it was prepared. One volume of trypsin solution was added to one volume of cell suspension, resulting in a cell density of 2.5×10^5 cells/ml

and a trypsin concentration of 0.25 μg/ml. Experiments were carried out at 20°C. The reaction was stopped by adding the cells to a tube on ice-containing relaxing solution with leupeptin, PMSF, and DIFP to a final concentration of 0.25, 0.5, and 5 mM, respectively. Cells were then solubilized and electrophoresed.

When the effect of trypsin on passive tension and stiffness was studied, cells were stretched by 50% in 10 s, and 2 s later passive tension and stiffness were measured at the extended length. Cells were released back to the slack length, and this protocol was repeated each several min for at least 30 min. This protocol was different from the one described in Protocols because it could be repeated more frequently, thus allowing us to study the time course of passive tension and passive stiffness change with higher time resolution. Leupetin was removed by flushing 50 ml of leupeptin-free relaxing solution through the chamber, and passive tension and stiffness were measured again for 30 min. Trypsin was added by flushing 36 ml of trypsin (0.25 μg/ml)--containing relaxing solution through the chamber, and the time course of tension and stiffness change was determined.

Thick filament depolymerization

To obtain a slow and controlled mode of depolymerizing the ends of the thick filaments, cells were incubated in a relaxing solution that contained 180 mM KCl instead of the 70 mM K-proprionate that was normally present. This increased ionic strength from 180 to 290 mM (calculated according to Fabiato, 1988). Cells were incubated in this solution (10^5 cells/ml), and after the desired time the reaction was stopped by adding to the cells a 12-fold excess of normal relaxing solution. This decreased the ionic strength to about 0.188 M. Cells were studied by optical microscopy to measure their A-band widths, and by SDS-PAGE to study their protein composition.

Microtubule depolymerization

Tsutsui et al. (1993; 1994) have successfully used both low temperature and colchicine to depolymerize microtubules from intact myocytes. To stay close to their protocols, we initially tried to work with intact myocytes, but were not successful in gluing these cells to the transducers because contact with the glue activated and severely shortened the cells. Skinned cells were therefore used. Because unpolymerized tubulin and free proteins involved in microtubule stability (for review, see Rappaport and Samuel, 1988) are likely to diffuse out of Triton-skinned cells, initial experiments were carried out with Triton X-100 skinned cells using as relaxing solution the microtubule-stabilizing buffer of Schliwa et al. (1981), modified by adding 2 mM MgATP. Protocols consisted of first measuring passive tension and stiffness in this buffer at 20°C and then depolymerizing the microtubule by cooling the cells to 4°C for 3 h (cf. Samuel et al., 1983) and measuring passive tension and stiffness again after rewarming to 20°C. These experiments were not successful, in that the cells tended to go into rigor in this microtubule-stabilizing buffer, despite the presence of 2 mM MgATP.

We finally settled on the following protocol. Cells were skinned with α-toxin, a skinning agent that makes small pores in the plasma membrane, large enough to allow passage of ions and small molecules such as ATP and EGTA, but much too small to allow proteins such as unpolymerized tubulin or proteins involved in microtubule stability to diffuse out of the cells (Kitazawa et al., 1989; Sweitzer and Moss, 1993). We believe that it is unlikely, therefore, that the polymerization state of the microtubules was altered by α-toxin-based skinning. Skinned cells were first mechanically characterized by stretching the cells by 40% in 180 s and then releasing them with the same velocity while measuring passive tension and stiffness. This protocol was repeated every 20 min for a total duration of 2–3 h. Relaxing solution was then added that contained 1.0 μM colchicine (Sigma, C-9754), and its effect on tension and stiffness was investigated. This concentration has been shown to be an optimal concentration for depolymerizing microtubules in heart cells (Tsutsui et al., 1993). Initially, experiments were carried out at 37°C to mimic the experimental conditions of the study of Tsutsui et al. (1993), but passive tension of control cells typically decreased somewhat with time, and the preparations were not stable enough for this type of experiment. Experiments were therefore carried out at 20°C, where mechanical properties of control cells were reproducible for periods exceeding 10 h.

Statistics

The results of our studies will be given as the mean ± SE, unless indicated otherwise. Significant differences were assigned to selected parameters using the Student's t-test with $p < 0.05$.

RESULTS

Titin in rat cardiac muscle

Cardiac titin from the rat was studied using SDS-PAGE. To obtain high molecular mass protein standards, we co-electrophoresed samples from psoas and semitendinosus muscle from the rabbit, and insect indirect flight muscle (IFM) from Lethocerus. Fig. 2 *A* shows that cardiac T1 migrates much further on gels than T1 from skeletal muscle. To estimate the molecular mass of cardiac T1, a calibration curve was constructed using the following literature values for molecular mass: T1 and nebulin of semitendinosus muscle, 2.94 and 0.78 MDa; T1 and nebulin of psoas muscle, 2.80 and 0.70 MDa; T2 of psoas and semitendinosus, 2.1 MDa (Kruger et al., 1991; Wang et al., 1993). The calibration curve so obtained (Fig. 2 *B*) predicted a molecular mass of 2.49 ± 0.03 MDa for rat cardiac T1. A similar value has been reported for rabbit cardiac titin (Wang et al., 1991). It should be stressed that due to absence of non-titin high molecular mass standards, we cannot be absolutely certain of the exact molecular mass of the titin isoforms.

The relative amount of titin was determined by measuring the ratio between the amounts of titin and myosin heavy chain (MHC). In rat heart muscle, this ratio was on average somewhat higher than in rabbit skeletal muscle (Table 1), but the difference was not significant ($p = 0.05$). The main difference between rat cardiac muscle and skeletal muscle titin is that cardiac titin has a lower molecular mass.

Because of the lower molecular mass of cardiac titin, the extensible titin segment in the I-band is predicted to be only 0.19 μm when unstrained, which is 0.1–0.2 μm shorter than in skeletal muscle (See Table 1 and Discussion). The I-band strain of titin is the fundamental determinant of the amount of passive tension that is generated (Granzier and Wang, 1993b) and, therefore, the much shorter extensible titin segment of cardiac muscle predicts that passive tension in cardiac muscle increases much steeper with sarcomere length than it does in skeletal muscle. Furthermore, a yield point (sarcomere length where passive tension reaches a plateau) is predicted at a sarcomere length of about 2.9 μm, which is much shorter than the yield points of skeletal muscle (Table 1).

In studying the mechanical properties of titin in cardiac muscle, it is important to ensure that the preparation that is being used contains undegraded titin, because titin is notoriously sensitive to proteolytic degradation (Granzier and Wang, 1993C). Fig. 2 *C* shows that when cells were isolated,

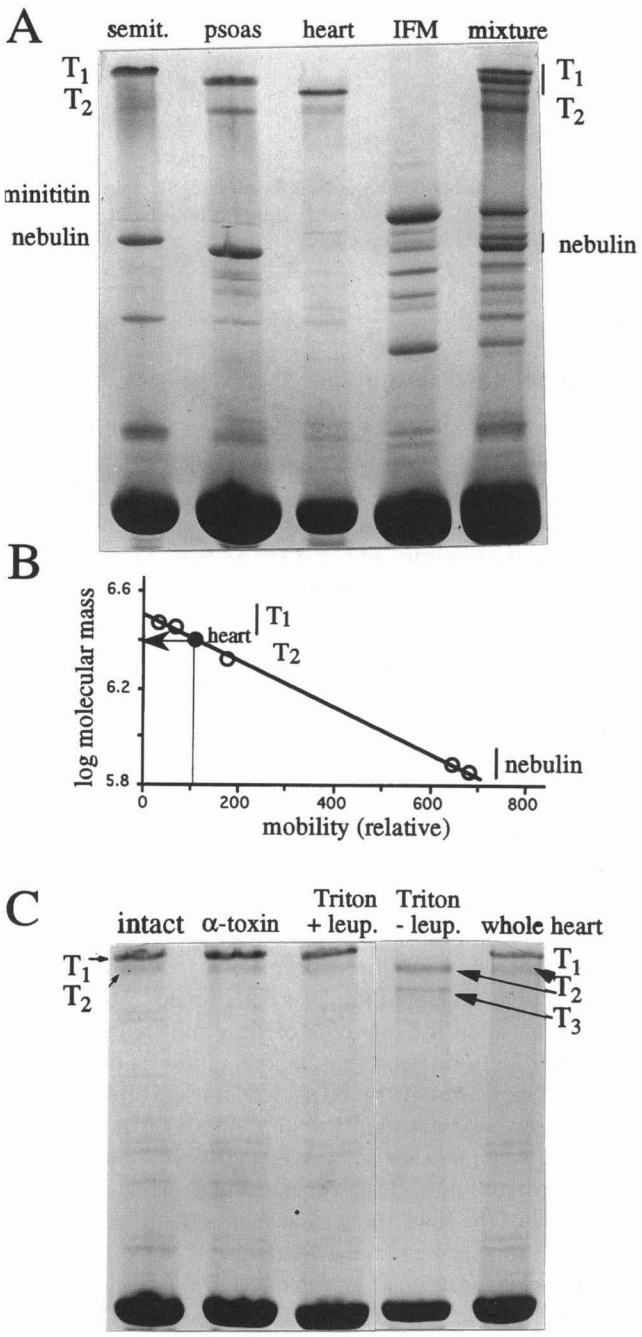

FIGURE 2 Titin in heart muscle. (*A*) SDS-PAGE-based comparison of titin from rat heart, skeletal muscle (semitendinosus and psoas from rabbit), and insect indirect flight muscle (IFM) from Lethocerus. T1 of the rat heart is much smaller than that of the skeletal muscle. This is most clear in the 5th lane, where the samples shown in the first four lanes were mixed (T1 of the heart is the third band from the top). (*B*) Estimation of molecular mass of cardiac T1. The relationship between migration distance and log molecular mass was determined using as standards the values reported in the literature for T1, T2, and nebulin of rabbit psoas and semitendinosus muscle (see text). The obtained linear relationship and the measured migration distance predicted a molecular mass of 2.49 MDa for cardiac T1. (*C*) Titin in skinned myocytes. Intact myocytes (lane 1) and myocytes skinned with α-toxin (lane 2) and Triton X-100 in the presence of leupeptin (lane 3) contain an amount of T1 that based on comparison with titin in the whole heart (lane 5) appears normal. However, when myocytes were skinned without leupeptin (lane 4), T1 was completely degraded, and a new band appeared below T2, which we named T3.

TABLE 1 Comparison of titin from cardiac and skeletal muscle

	Skeletal muscle*		Cardiac muscle (rat)
	Semi-tendinosus	Psoas	
Molecular mass (MDa)‡	2.94	2.80	2.49 ± 0.01
Contour length of titin§			
total (μm)	1.176	1.120	0.99 ± 0.005
extensible segment (μm)	0.376	0.320	0.19 ± 0.005
"Yield" point (μm)¶	4.6	3.6	**2.93 ± 0.04**
Titin/MHC ratio	0.19 ± 0.02	0.21 ± 0.04	0.27 ± 0.04
Titin filaments/ half thick filament‖	5.0 ± 0.6	5.9 ± 1.2	8.2 ± 1.2

*From rabbit.

‡Data for skeletal muscle taken from Wang et al. (1991) and used as standards to estimate the molecular mass of cardiac titin (see Fig. 2). The measurements from our study are given as mean ± SE.

§Total length estimated by assuming that the linear mass of titin is 2.5 MDa/μm, and the length of the unstrained extensible segment in the I-band estimated by subtracting the half A-band width (1.6 μm) from the total (cf. Wang et al., 1991).

¶Yield point defined as the sarcomere length at which passive tension reaches a plateau. The values for skeletal muscle are taken from Granzier and Wang (1993b). The strain of the extensible titin segment is about 3.5 at the yield point in skeletal muscle. Assuming that a sarcomere length yield point is found in cardiac muscle at a similar extensible titin strain, then the predicted yield point is as shown in bold.

‖Assuming 150 myosin molecules per half thick filament (Squire, 1986).

washed and skinned as described in Materials and Methods, titin was not degraded. It was critical, however, to include the protease inhibitor leupeptin in the skinning solution. When leupeptin was left out, T1 was found to be completely degraded into T2 and into a newly appearing band, about 200 kDa smaller than T2, that we named T3 (Fig. 2 *C*).

Tension in passive single myocytes

Passive tension of cardiac cells was found to increase continuously, initially steeply and at longer lengths more slowly (Fig. 3 *A*, curve marked "total"). During release, passive tension was less than during stretch, indicating hysteresis. Hysteresis was severe when long sarcomere lengths were reached during stretch (~4.5 μm), but much less when sarcomeres were stretched to a more modest length (Fig. 3 *A*).

The cells used in this study were normally isolated in the presence of BDM, to prevent shortening during cell separation. To test whether BDM affected passive tension, cells were also isolated without BDM, and the cells were first studied in normal relaxing solution and then in relaxing solution that contained 15 mM BDM. BDM affected neither passive tension nor passive stiffness (Fig. 3), in agreement with results reported by Linke et al. (1994).

It was surprising that the passive tension-sarcomere length curves did not display a plateau at long lengths, as occurs in skeletal muscles. It is known from previous work (Wang et al., 1993; Granzier and Wang, 1993b) that the tension plateau in skeletal muscle only occurs over a limited sarcomere length range, beyond which tension starts to increase

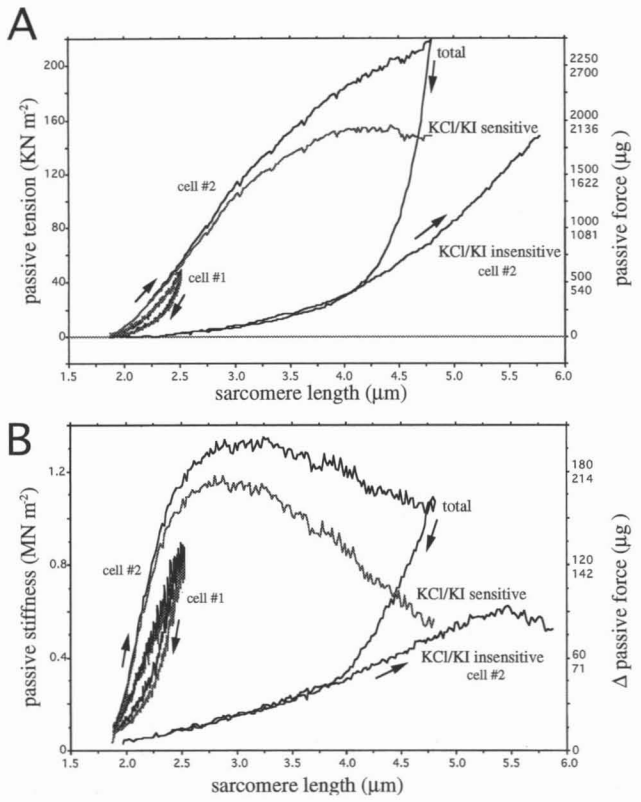

FIGURE 3 Passive tension, sarcomere length (*A*), and passive stiffness, sarcomere length (*B*), relations of single myocytes isolated from the right ventricle. Cells were stretched with a constant sarcomere velocity (0.005 μm/s) from their slack length to either a sarcomere length of 2.5 μm (cell #1) or of 4.7 μm (cell #2), after which the cell was released with the same velocity back to the slack length. Stiffness was measured using brief bursts of 70-Hz sinusoidal oscillations, which were repeated every 350 ms. The cell that was stretched to 2.5 μm (cell #1) was isolated without BDM, and passive tension was measured in normal relaxing solution (*dark line*) and in relaxing solution (*light line*) containing 15 mM BDM (incubation time 25 min). Note: for cell #1 two stretch/release loops are superimposed, but the two loops are virtually indistinguishable. This indicates that BDM does not affect passive tension. The cell that was stretched to a length of 4.7 μm had been isolated using BDM as explained in Materials and Methods. First, the control curve was measured, after which the cell was treated with KCl/KI (see text), and the KCl/KI-insensitive component was then measured by stretching the cell using the same velocity as before. By subtracting the KCl/KI-insensitive component from the total before treatment, the KCl/KI-sensitive tension and stiffness were obtained. The right-hand scales show results in μg; the numbers at the bottom apply to cell #1 and at the top to cell #2. For the left-hand scales, these values have been converted to tension and stiffness.

again because of the tension contribution from intermediate filaments at lengths longer than about 5 μm. Because cardiac muscle contains severalfold more intermediate filament proteins (e.g., desmin) than skeletal muscle (Price, 1984), we decided to test whether absence of a tension plateau in myocytes resulted from intermediate filaments that contribute to passive tension at much shorter lengths than 5 μm, thereby masking the plateau of the titin-based passive tension.

The intermediate filament system was studied by treating the cells first for 10 min with relaxing solution that contained an additional 0.6 M KCl, and then for 30 min with relaxing solution that contained 1.0 M KI (cf. Granzier and Wang, 1993b). This treatment removed actin and myosin to levels less than 5% of the controls (results not shown). It is known from work by others (Price, 1984; Roos and Brady; 1989) that similarly extracted cardiac preparations still contain their intermediate filament systems.

After KCl/KI treatment, passive tension was much reduced, but it was not completely absent, not even at lengths close to the slack length. It is also worth noting that the tension curves after KCl/KI treatment were reproducible. When the KCl/KI-insensitive tension was subtracted from the total tension, KCl/KI-sensitive tension was obtained that did reach a plateau at long lengths (Fig. 3 *A*).

We studied whether cells from left and right ventricles had different properties and found that none of the parameters measured (Table 2) were significantly different ($p = 0.05$). We therefore pooled data from all cells and determined their average properties (Table 2, last column; Fig. 4 *A*). In all cells, it was found that the initial increase in passive tension from a sarcomere length of about 2.1 to 2.5 μm could be fitted to the same exponential equation that fits this relation in skeletal muscle fibers (Sten-Knudsen, 1953; Granzier et al., 1991): $\sigma = E_0\alpha^{-1}(e^{\alpha\epsilon} - 1)$, where σ = passive tension and ϵ = sarcomere strain. The obtained exponent of exponential tension rise, α, was 11.9 ± 0.7 ($n = 10$), and the initial elastic modulus, E_0, was 26 ± 5.5. These values are severalfold higher than those reported for rabbit skeletal muscle (Granzier and Wang, 1993b). Passive tension in cardiac cells thus increases much more steeply with sarcomere length than in rabbit skeletal muscle.

Pooled results of all cells after KCl/KI treatment are shown in Table 2 and Fig. 4 *A*. At a sarcomere length of about 2.0 μm, KCl/KI-insensitive passive tension was 12.8 ± 4.2% ($n = 10$) of the pretreatment value, and at 4.0 μm this percentage had increased to 24 ± 3.4% ($n = 10$). It is this tension that makes the total passive tension increase continuously with sarcomere length (Fig. 4 *A*).

The passive tension that remains after the intermediate filament component is subtracted from the total measured tension, the KCl/KI-sensitive tension, initially increased steeply with sarcomere length and finally reached a plateau. The plateau tension was on average 118 ± 9 kN/m^2 ($n = 10$), or 2.05 ± 0.16 mg/cell, severalfold higher than the reported maximal active tension of rat myocytes (Sweitzer and Moss, 1993). The yield-point was found at 4.07 ± 0.09 μm ($n = 10$), which is much longer (>1 μm) than where the plateau is predicted based on the low molecular mass of cardiac titin (Table 1).

We investigated the possibility that the discrepancy between measured and predicted yield-point resulted from sarcomere length inhomogeneity. The real yield-point might indeed be at 2.94 μm, but measured tension could have increased beyond this length because there is a population of short sarcomeres that had not reached 2.94 μm. Because the tension at 2.94 μm is about half-maximal (Fig. 4 *A*), the

TABLE 2 Comparison of myocytes isolated from right and left ventricles

	Right ventricle (n = 5)	Left ventricle (n = 5)	p-value*	Left + right ventricle (n = 10)
Slack length (μm)	1.88 ± 0.04	1.91 ± 0.03	0.56	1.90 ± 0.03
Area at slack (μm^2)	182 ± 37	166 ± 25	0.73	174 ± 21
Passive tension‡				
α total§	12.2 ± 0.86	11.6 ± 1.2	0.70	11.9 ± 0.7
α KCl/KI-sensitive§	15.2 ± 2.2	11.0 ± 1.0	0.12	12.9 ± 1.3
α KCl/KI-insensitive	1.5 ± 0.1	1.3 ± 0.1	0.20	1.4 ± 0.1
E_0 total§ (kN/m^2)	20.6 ± 4.6	31.5 ± 10.2	0.36	26.0 ± 5.5
E_0 KCl/KI-sensitive§	15.8 ± 6.4	30.3 ± 10.1	0.26	23.0 ± 6.1
E_0 KCl/KI-insensitive	7.5 ± 1.9	10.8 ± 2.1	0.28	9.2 ± 1.5
KCl/KI-sensitive passive tension				
Yield length (μm)	4.19 ± 0.11	3.94 ± 0.13	0.18	4.07 ± 0.09
Yield tension (kN/m^2)	118.4 ± 10.9	117.0 ± 16.0	0.94	117.6 ± 9.1
KCl/KI-sensitive passive stiffness				
Yield length (μm)	2.84 ± 0.05	2.76 ± 0.05	0.95	2.80 ± 0.03
Yield stiffness (MN/m^2)	0.80 ± 0.16	0.83 ± 0.19	0.91	0.82 ± 0.12

Data given as mean ± SE.

*Based on Student's t-test.

‡Passive tension (σ): sarcomere strain relation (ϵ) fitted to $\sigma = E_0\,\alpha^{-1}\,(e^{\alpha\epsilon} - 1)$. ϵ range for total and KCl/KI-sensitive tension 0.1–0.3 and for KCl/KI-insensitive tension 1.0–2.0.

§Total: KCl/KI-insensitive component included; KCl/KI-sensitive: KCl/KI-insensitive component subtracted from total tension.

population of short sarcomeres has to contain about half of all sarcomeres in the cell, and their length has to be slack (~1.9 μm).

We estimated axial sarcomere length inhomogeneity from the fourier transform of the ROIs and, by determining the width of the power peak at half maximum (FWHM), deconvoluted by the fourier transform of the width of the ROI (see Materials and Methods). A total of 48 ROIs were investigated in 10 cells. The axial inhomogeneity estimate so obtained increased with sarcomere length and was 0.16 ± 0.02 μm when the tension yield-point (4.09 μm) was reached. These values were too small to explain the large discrepancy between the measured and predicted yield point.

Transverse sarcomere length inhomogeneity was estimated from the mean sarcomere length of ROIs that were located at different distances from the edge of the cells. We studied 53 ROIs in 10 cells at a length where passive tension was 50% of maximal. The mean sarcomere length so obtained was 2.85 μm, and its SD was 0.28 μm. Assuming that sarcomere length followed a normal distribution allows us to predict that less than 0.5% of all sarcomeres will be as short as 1.9 μm, which is about 100-fold less than required. It is thus unlikely that the measured yield-point was so much longer than predicted solely as a result of sarcomere length inhomogeneity.

Stiffness in passive single myocytes

Fig. 3 *B* shows an example of cells in which passive stiffness was measured as a function of sarcomere length, Table 2 shows that stiffness properties of cells from left and right ventricles were statistically indistinguishable, and Fig. 4 *B* shows the averaged results from 10 cells. Stiffness increased initially steeply with sarcomere length, and the increase from about 2.0 to 2.5 μm could be fitted by an exponential equation, confirming the observations of Brady and Farnsworth (1986). At lengths longer than about 2.5 μm, the increase in stiffness leveled off and stiffness reached a maximum at a length of about 3 μm and declined somewhat at longer lengths (Figs. 3 *B* and 4 *B*).

After KCl/KI treatment, passive stiffness was much reduced, but there was still a clearly measurable amount of stiffness remaining (Figs. 3 *B* and 4 *B*). Similar findings have been reported by Brady and Farnsworth (1986). The KCl/KI-insensitive stiffness was subtracted from the total stiffness, and the resulting KCl/KI-sensitive stiffness component reached a peak value at a sarcomere length of 2.80 ± 0.05 μm (n = 10) and then declined (Figs. 3 *B* and 4 *B*). When passive stiffness was plotted versus passive tension, very different relations were obtained for KCl/KI-insensitive and KCl/KI-sensitive stiffness, with KCl/KI-insensitive stiffness being much lower for a given amount of tension (Fig. 4 *C*). This suggests that KCl/KI-sensitive and -insensitive stiffness are derived from different sources. In the discussion, we show that these sources are likely to be titin and intermediate filaments, respectively.

Effect of trypsin-based titin degradation on tension and stiffness

Myocytes were digested with trypsin (0.25 μg/ml at 20°C) for a range of incubation times, the reaction was stopped, and cells were solubilized and electrophoresed (Fig. 5 *A*). Almost immediately after trypsin was added, T1 decreased in intensity, whereas T2 increased. A few minutes later, two new bands appeared, one just below T2, which we named T3, and the other just below myosin heavy chain. Quantitative densitometry revealed that only titin was clearly affected by trypsin whereas, for example, myosin was not (Fig. 5 *B*). T1 was found to disappear to an undetectable level within 30 min

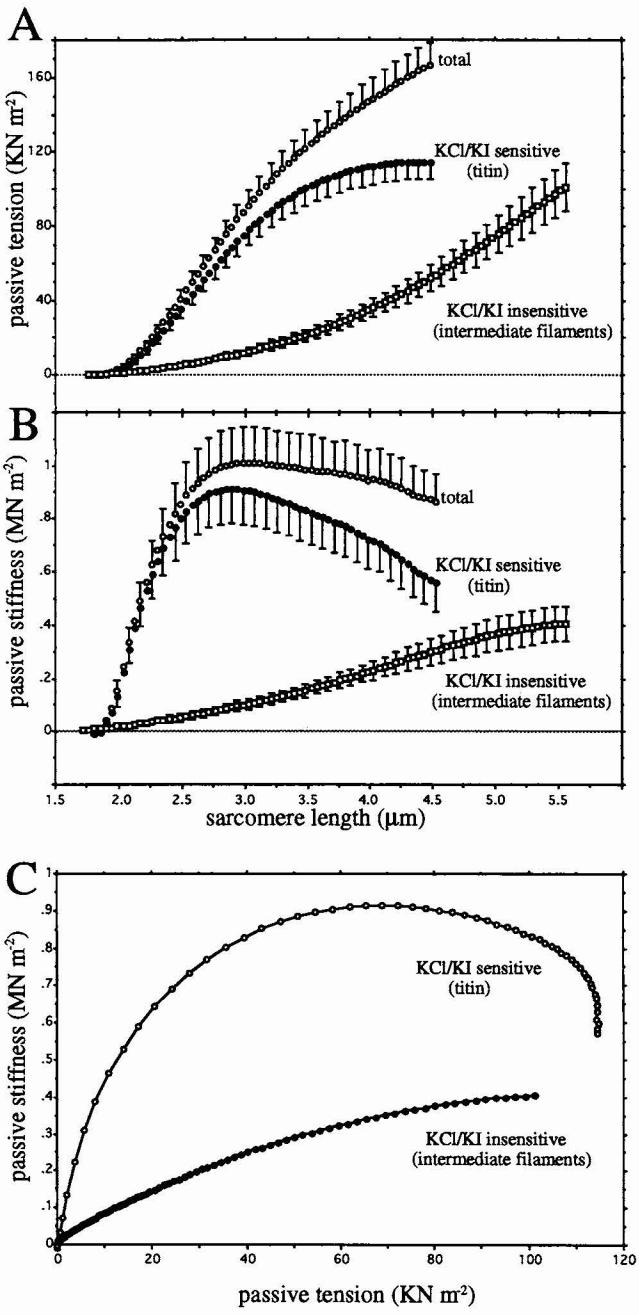

FIGURE 4 Passive tension and passive stiffness in cardiac myocytes. (*A*) Passive tension-sarcomere length relation. (*B*) Passive stiffness-sarcomere length relation. (*C*) Passive stiffness-passive tension relation. Mean values and SEs of the mean of 10 myocytes are shown in *A* and *B* and only mean values in *C*. For clarity, only the stretch parts of the stretch-release cycles are displayed. For further details, see text and the caption of Fig. 3.

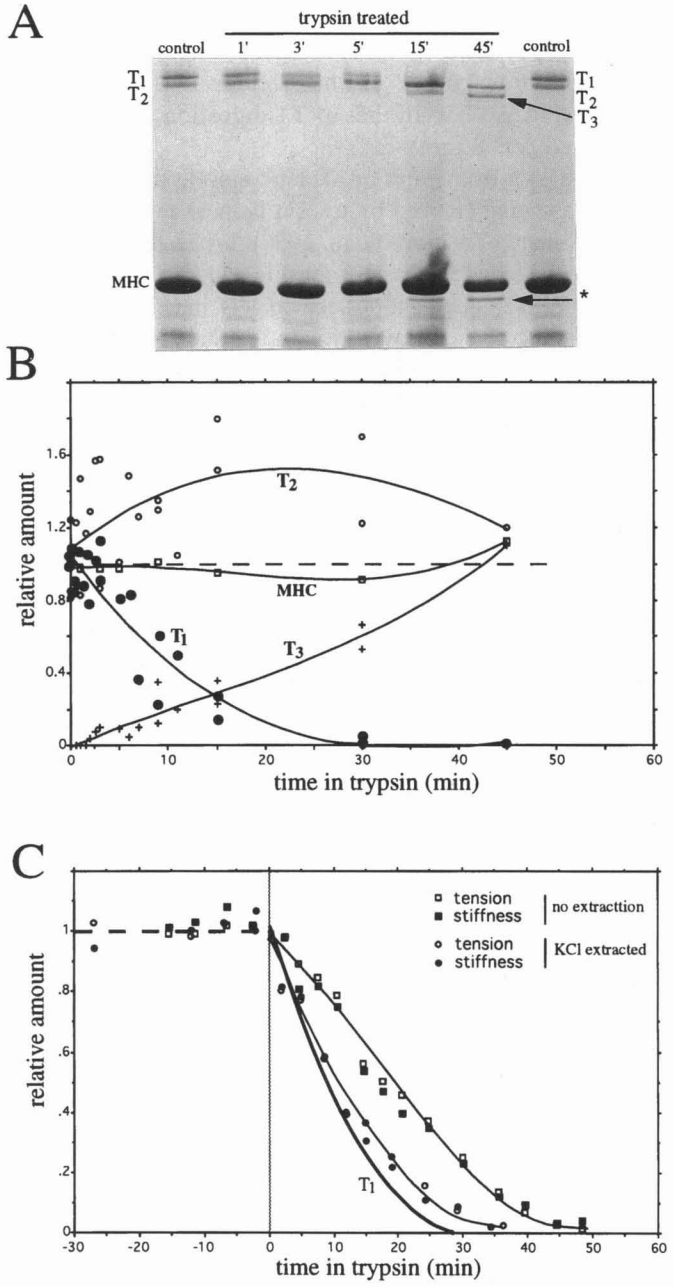

FIGURE 5 Effect of trypsin on protein content, passive tension, and passive stiffness. (*A*) SDS-PAGE of cells treated with trypsin. T1 disappears, and a new band appears below T2 (T3) and one just under MHC (see *asterisk*). (*B*) Quantitative densitometry of cells treated with trypsin. The amount of protein is expressed relative to that of untreated cells, except for T3, which is only present after trypsin treatment and for which absolute peak areas (OD × pixels) are given that were not normalized. Note that MHC does not appear to be affected by trypsin. Lines are third-order polynomial fits to the data. (*C*) Effect of trypsin on tension and stiffness of passive cells. Open and closed circles are from cells that had first been treated for 1 h with a high KCl solution that depolymerized some 60% of the ends of the thick filament (see below). Tension and stiffness fell faster in the KCl-extracted cells than in the control cells (□ and ■), and both are close to the measured decrease of T1 (for which for clarity, only the third-order polynomial fit to the data is shown as the *thick solid line*).

of digestion, with a $T_{1/2}$ of ~8 min. T2 increased initially, and later decreased by a modest amount, probably as a result of the initial conversion of T1 into T2, and the later conversion of T2 into T3.

Passive tension and stiffness were measured while cells were being digested with trypsin. Cells were stretched by 40% in 10 s, held at the extended length for 2 s, tension and stiffness were measured, and cells were then released back to the slack length. This protocol was repeated every few minutes, and results were plotted as a function of the incubation time in trypsin (Fig. 5 *C* curves marked "no

extraction"). It was found that immediately after the addition of trypsin, tension and stiffness decreased. However, the time course of the decrease was somewhat slower (Fig. 5 *C*) than that of T1 digestion seen on gels ($T_{1/2}$ = 22 vs. 8 min).

It is known from work on skeletal muscle that the site in T1 that is being cleaved by trypsin is localized at the edge of the A-band (Yoshioka et al., 1986). We tested, therefore, whether the slow decrease of tension and stiffness, relative to that of the T1 degradation seen on gels, may have resulted from binding of the cleaved titin to the thick filament. This would allow cleaved titin to still develop some tension and stiffness until additional digestion took place, for example, from T2 into T3.

Experiments were conducted in which the ends of the thick filament were slowly depolymerized using a moderately high ionic strength relaxing solution (cf. Roos and Brady, 1989) that contained 180 mM KCl instead of the 70 mM K-proprionate normally present. The extent of thick filament depolymerization was estimated by both A-band width measurements using optical microscopy and by measuring the MHC content using SDS-PAGE. It was found that upon the addition of high KCl relaxing solution, both the A-band width and the MHC content decreased in about 10 min to 50% and then decreased much slower, reaching 60–70% extraction in about 60 min (Fig. 6). A small amount of T1 (10–15%) was also removed by this extraction protocol (Fig. 6).

Passive tension and stiffness were also measured during thick filament depolymerization. Both fell somewhat during the 60-min incubation time in high KCl relaxing solution, but only by a modest amount (20–30%). The significance of this finding will be further addressed in Discussion.

After extracting the A-band for 60 min with high KCl, the cells were washed with normal relaxing solution (leupeptin-free) and were then treated with trypsin. It was found that both tension and stiffness fell more rapidly then in unextracted cells, with a time course that was very close to the disappearance of T1 as measured with SDS-PAGE (Fig. 5 *C*). We conclude that the relatively slow decrease of tension and stiffness measured in unextracted cells most likely resulted from binding of the cleavage products of titin to the thick filament. The similarity between the time course of decrease of tension and stiffness, and the time course of T1 disappearance, is in agreement with titin being a major contributor to passive tension in cardiac myocytes.

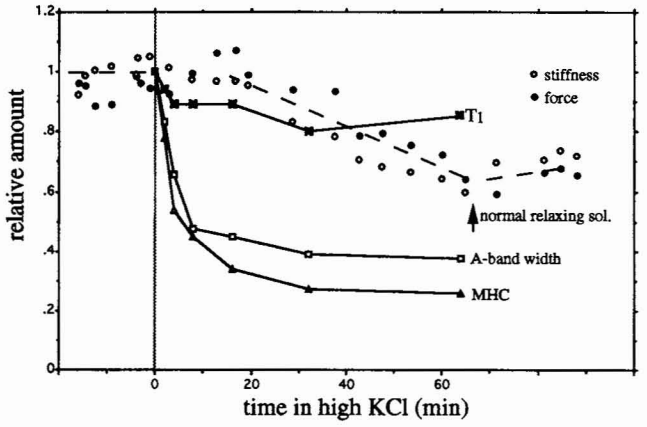

FIGURE 6 Effect of high KCl relaxing solution on A-band width, protein content (MHC and T1), and passive tension and stiffness. Both A-band width and MHC content initially fell rapidly and then more slowly until they reached 60–70% extraction after 60 min. A small amount of T1 (10–20%) is also extracted after 60 min in high KCl. Tension and stiffness were measured 2 s after the cells had been stretched in 10 s from their slack length to about 2.7 μm. Tension and stiffness fell by about 20–30% after 60 min in high KCl. See text for further details.

Effect of colchicine on passive tension and stiffness

Microtubules have been shown to mechanically obstruct sarcomere shortening in the activated hypertrophied myocardium (Tsutsui et al., 1993, 1994). We investigated whether microtubules contribute to the passive mechanical properties of cardiac cells upon stretch. All studies described in the previous sections were carried out on cells that had been skinned with Triton X-100 and that had been kept subsequently for 3 h at 0–4°C, which is known to depolymerize microtubules (Rappaport and Samuel, 1988). This assured us that microtubules did not contribute to the mechanical properties that we measured. To investigate the possible role of microtubules in passive tension development, cells were used that had been skinned with α-toxin and that were not cooled below room temperature. These cells were used immediately after they had been isolated. Passive tension and stiffness of these cells were measured repeatedly over a period of several hours, after which relaxing solution was added that contained colchicine.

It was found that cells responded to colchicine in a variable fashion. Some cells did not seem to be affected by colchicine (Fig. 7 *A*). In other cells, there was during the first 60 min of colchicine incubation a clear drop in tension and stiffness after which both leveled off to a new steady level. In principle, this decrease in tension and stiffness could have resulted from a slight decrease in sarcomere length due to slippage of the cell attachment to the transducers. Careful comparison of the sarcomere lengths at which the cells were when tension and stiffness were measured before and during colchicine treatment revealed that the sarcomere lengths were not different (results not shown). Changes in sarcomere lengths that were smaller than the resolution of our detection method (~40 nm) would have gone undetected. Assuming that such undetected changes occurred, and that they went in the right direction, we estimated the ensuing drop in tension and stiffness, using the measured control curves. It was found that a 40-nm length change could have accounted for 45 ± 5% of the observed tension decrease and for 25 ± 5% of the observed stiffness decrease. It is thus unlikely that changes in sarcomere length during the colchicine treatment were solely responsible for the effect of colchicine on tension and stiffness that was observed in some cells.

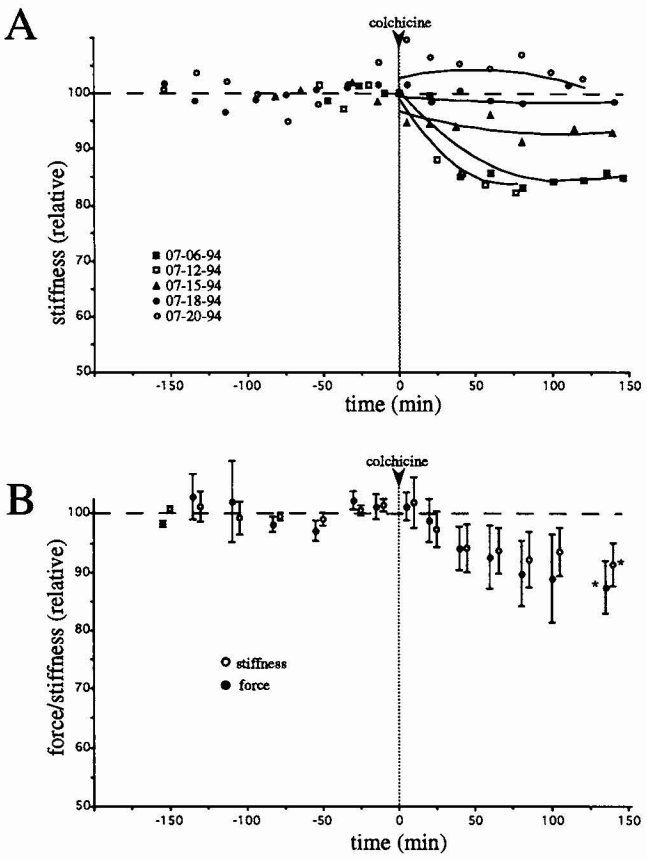

FIGURE 7 Effect of colchicine on tension and stiffness. Tension and stiffness were measured at the end of a 30% stretch completed in 90 s. The cells were then released, and the protocol was repeated about every 20 min. At $t = 0$ min, 1 μM colchicine was added. (*A*) Result of five individual cells. For clarity, only passive stiffness is shown (passive tension had a little bit more scatter but behaved otherwise similar to stiffness). Some cells showed an initial drop in stiffness and then attained a steady value. Other cells were not affected by colchicine. (*B*) Average results of all cells. Data were grouped in time bins, and the mean and standard errors were plotted. Only those results indicated with an asterisk had decreased from the control levels in a significant manner ($p = 0.05$).

When all cells were averaged, a 10% decrease of tension and stiffness over a period of about 60 min was obtained, after which tension and stiffness stayed more or less constant (Fig. 7 *B*). However, most of this decrease in the presence of colchicine was not significant ($p = 0.05$). It appears that although the contribution of microtubules to passive tension and stiffness of individual cells can be substantial, their average contribution is modest at best.

We also tested whether after the colchicine treatment, passive tension was affected by skinning cells with Triton. It was found that within seconds after the addition of 0.5% Triton X-100, striations in the cells became much clearer, probably as a result of the dissolution of mitochondria. After skinning for 30 min, and then extensive washing with normal relaxing solution, passive tension and passive stiffness (measured as in Fig. 7) were 94.0 ± 3.4% ($n = 5$) and 99.4 ± 0.7% ($n = 5$) of the pre-Triton values. It appears that passive properties are not affected by Triton.

Passive tension in rat trabeculae

To investigate to what degree extracellular structures (collagen) determine the passive properties of cardiac muscle, we studied the passive tension-sarcomere length relations of trabeculae. Trabeculae were stretched with a sarcomere velocity of 0.005 μm/s and then released with the same speed, exactly as we had done earlier on the isolated cells.

The passive tension-sarcomere length relations of the trabeculae were only reproducible if sarcomere length did not exceed about 2.2 μm, and the sarcomere length range was thus limited from the slack length (~1.90 μm) to 2.2 μm, a range that is close to the working range of the heart (Rodriguez et al., 1992). Passive tension of the trabeculae was found to increase very slowly for the first 0.2 μm of sarcomere stretch, and then much faster (Fig. 8 *A*, control curve). The transition between slow and fast tension rise

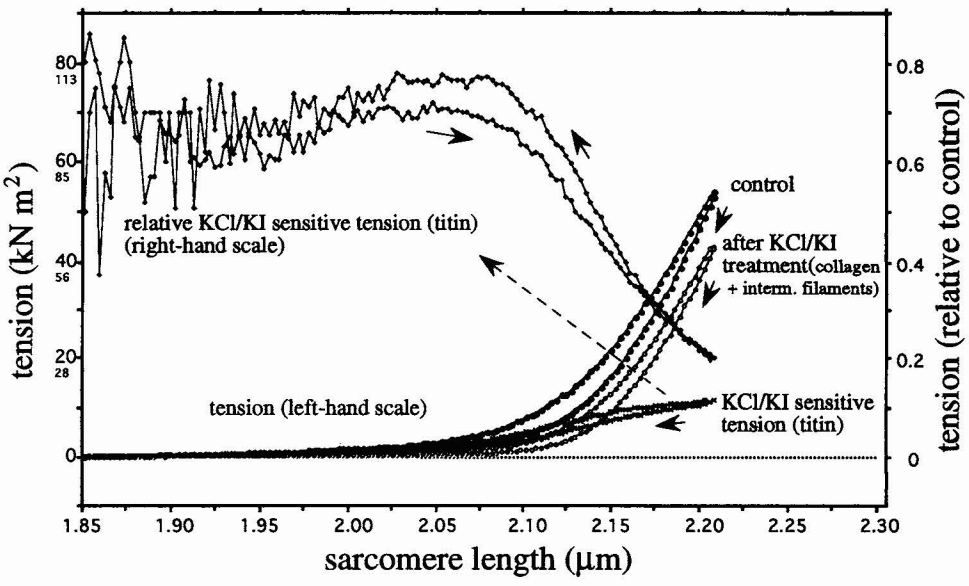

FIGURE 8 Example of passive tension-sarcomere length relation of a skinned trabeculae. The control curve was obtained by stretching the preparation with a sarcomere velocity of 0.005 μm/s. The preparation was then released back to the slack length and treated for 20 min with relaxing solution containing 0.6 M KCl followed by 45 min with relaxing solution containing 1 M KI. Passive tension was then measured again, using the exact same protocol as before: see curve labeled "after KCl/KI treatment." The KCl/KI-sensitive tension, obtained by subtracting the curve after the treatment from the control curve, was plotted both on an absolute scale (left-hand scale) and on a relative scale by dividing the values by the control tensions (right-hand scale). Small numbers on the left-hand scale show the results as passive force (in mg). See text for further details.

could be easily determined by plotting the logarithm of passive tension versus sarcomere length. This indicated that the fast rise started at 2.08 ± 0.01 μm (n = 6).

Trabeculae were incubated for 20 min in relaxing solution with 0.6 M KCl and then for 45 min in relaxing solution with 1 M KI. This removed the majority of myosin (98.4 ± 1.3%) and actin (94.6 ± 4.6%), while their associated proteins (e.g., C-protein, α-actinin, troponin, and tropomyosin) were removed to undetectable levels. Also titin was extracted, by 89.1 ± 6.9% (n = 6). It is thus likely that the KCl/KI treatment of the trabeculae abolished titin as major intracellular source of passive tension because titin was largely removed, and because its anchor points in the sarcomere had disappeared.

After the KCl/KI treatment, tension was lower, but the general shape of the passive tension-sarcomere length curve was not affected (Fig. 8). The KCl/KI-sensitive tension was obtained by subtracting tension after KCl/KI treatment from the control values, and Fig. 8 shows that the obtained KCl/KI-sensitive tension increased gradually with sarcomere length without showing a sharp increase as was observed in the control curves. We also determined the KCl/KI-sensitive tension relative to that of the control curves and found that from the slack length to about 2.05 μm, this tension was about 70% of the control values, whereas at longer lengths it decreased sharply (Fig. 8, right-hand scale).

Passive tensions measured during the release of the stretch/release loops were somewhat lower than during stretch, i.e., the trabeculae showed a small amount of hysteresis. Hysteresis had a modest effect on the relative KCl/KI-sensitive tension. This relative tension was slightly higher (on average 5%) during release than during stretch (Fig. 8).

Fig. 9 *A* shows the averaged results of trabeculae and myocytes. The KCl/KI-sensitive tension of trabeculae (*filled circles*) is remarkably close to that of the myocytes (*crosses*), and the small differences that existed at some sarcomere lengths were found to be statistically insignificant. KCl/KI treatment removed about the same amount of tension from trabeculae as from myocytes, indicating that the KCl/KI treatment on trabeculae did not affect the tension potential of extracellular structures.

The KCl/KI-insensitive tension of the trabeculae was much higher than that of cells, indicating that this tension was partially localized extracellularly. Because we did not have a means of experimentally dissecting the intracellular and extracellular component of the KCl/KI-insensitive tension of

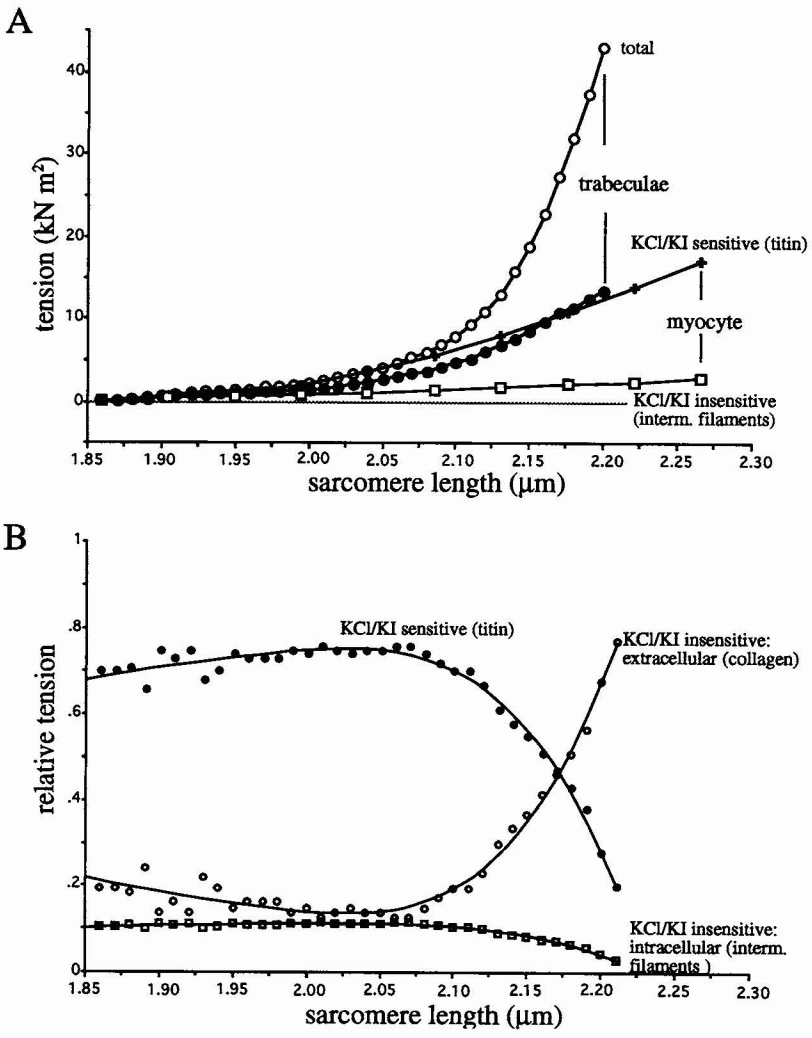

FIGURE 9 (*A*) Comparison of passive tension obtained from trabeculae and single myocytes measured with identical stretch/release protocols. Total tension (○) and KCl/KI-sensitive tension (●) obtained from six trabeculae are plotted (for clarity, only mean values are shown). Superimposed is the KCl/KI-sensitive tension (*crosses*) and the KCl/KI-insensitive tension (□) of myocytes (mean values of 10 myocytes). (*B*) Relative contribution of extracellular and intracellular KCl/KI-insensitive tension and KCl/KI-sensitive tension to the total passive tension of trabeculae. See text for further details.

trabeculae, we assumed that the same intracellular component measured for the myocytes existed in the trabeculae. By subtracting this component from the total KCl/KI-insensitive tension of the trabeculae, we calculated the KCl/KI-insensitive tension that was localized extracellularly. In this way, we dissected the KCl/KI-insensitive tension into two components. We determined their magnitudes relative to the total tension. The relative magnitude of the KCl/KI-sensitive tension was also determined.

The extracellular KCl/KI-insensitive tension was found to contribute about 20% of the total over a sarcomere length range from slack to 2.10 μm. At longer lengths, it rose sharply, to about 80% of the total at a sarcomere length of 2.20 μm. The intracellular KCl/KI-insensitive tension was about 10% of total tension from slack sarcomere length to about 2.10 μm, and its contribution then dropped to about 3% at 2.20 μm. Finally, the KCl/KI-sensitive component was at 70% of total tension from slack to about 2.10 μm, and then it dropped sharply to about 20% at 2.20 μm: Fig. 9 *B*.

DISCUSSION

We investigated the contribution of collagen, titin, microtubules, and intermediate filaments to tension and stiffness of passive rat cardiac muscle. We "dissected" their individual contributions by studying the effects of KCl/KI extraction on both trabeculae and single myocytes, the effect of trypsin digestion on single myocytes, and the effect of colchicine on myocytes. It was found that over the working range of the heart (sarcomere lengths ~1.9–2.2 μm), collagen and titin are the most important contributors to passive tension, with titin dominating at the shorter lengths of the working range and collagen at the longer lengths. Microtubules contributed modestly to passive tension in some cells but not in others. Finally, intermediate filaments contributed about 10% to passive tension at lengths from ~1.9 to 2.1 μm, after which their contribution dropped to only a few percent at ~2.2 μm.

Functional dissection

In this work, we set out to "dissect" the various structures that contribute to passive tension of cardiac muscle. An important tool that we used consisted of treating isolated myocytes and trabeculae with 0.6 M KCl, followed by 1 M KI. This treatment removed virtually all thick and thin filament proteins and also, to a lesser extent, titin. It is likely that the passive tension and stiffness drop that is caused by KCl/KI results from both removal of titin and from the lost of anchor points for titin in the sarcomere (thick filaments), thereby preventing it from developing tension (Wang and Ramirez-Mitchell, 1983). This conclusion agrees with the observation that mild trypsin treatment of the myocytes, which specifically digests titin (Fig. 5), removes about the same amount of passive tension as does the KCl/KI treatment. It therefore seems justifiable to equate the KCl/KI-sensitive tension of myocytes to the tension derived from titin.

The tension that remains in myocytes after KCl/KI treatment could in principle originate extracellularly, that is, from remnants of the collagen network. However, this is unlikely. Ultrastructural studies (reviewed by Brady, 1991) have documented that collagenase digestion of the heart results in myocytes that are free of collagen. In our study, isolated cells were treated, nevertheless, for a second time with collagenase using digestion conditions that are in themselves sufficient to digest the whole heart into myocytes (see Materials and Methods), thereby further decreasing the likelihood that myocytes still contained collagen. Furthermore, the KCl/KI-insensitive tension of myocytes increases only gradually with sarcomere lengths between 2.0 and 2.2 μm (Fig. 4) where collagen-based tension (see below) increases very steeply (Fig. 9). It is likely, therefore, that the KCl/KI-insensitive tension in our isolated myocytes is not collagen-based but has an intracellular source.

A good candidate for an intracellular source of this tension is the intermediate filament system. It has been reported that cardiac muscle contains a large amount of intermediate filament proteins (desmin) that resist KCl and KI extraction (Price, 1984), and that tension generated by the intermediate filament system in skeletal muscle does not seem to be affected by KCl/KI treatment (Wang et al., 1993; Granzier and Wang, 1993b). It thus seems reasonable to assume that the KCl/KI-insensitive tension of myocytes is derived from the intermediate filament system.

The KCl/KI-insensitive tension component in trabeculae is much larger than that of myocytes, a difference that is likely to result from extracellular structures contributing to passive tension. The extracellular matrix of cardiac muscle contains various filaments (microfibrils, elastic fibers, collagen fibers and fibrils, struts, etc.; see Robinson et al., 1983). Although it cannot be excluded that several of these types of filaments develop passive tension, because of its abundance and general distribution, collagen is the most likely candidate for an extracellular structure that develops passive tension (Brady, 1991a; Weber et al., 1994). By subtracting the KCl/KI-insensitive tension of the myocytes from that of the trabeculae, we were then able to determine the passive tension generated by collagen.

Finally, the contribution of microtubules to passive properties of cardiac cells was investigated with colchicine. This study rests on two main assumptions. The first one is that microtubules are still present in the skinned cells when the control curves are measured. Cells were skinned with α-toxin, which makes pores in the plasma membrane that only allow passage of low molecular weight solutes (e.g., ATP, EGTA, etc.) but not of high molecular weight (molecular mass > 4 kDa) solutes (Kitazawa et al., 1989). It is thus likely that free tubulin and proteins involved in microtubule stability (molecular mass 100 kDa and ~60–300 kDa, respectively; see Rappaport and Samuel, 1988) remain inside the cells. That α-toxin skinning does not disturb intracellular processes that require the presence of diffusable proteins is indicated by the finding that the receptor-coupled activation pathway is intact in α-toxin-skinned smooth muscle (Kitazawa et al., 1989). It therefore seems likely that the microtubular system in α-toxin-skinned cardiac cells is still

intact. The other main assumption is that during colchicine treatment microtubules indeed depolymerize. We believe that it is likely that this is the case because of various immunofluorescence studies by others on cardiac cells that have shown that colchicine, used at the same concentration as in our study, depolymerizes microtubules (for review, see Rappaport and Samuel, 1988; Tsutsui et al., 1993).

In conclusion, we believe that the experiments that we conducted did indeed allow us to "dissect" the contribution of collagen, titin, intermediate filaments, and microtubules to the passive properties of cardiac muscle.

Collagen

It was found that collagen contributes to passive tension over the whole working range of sarcomeres in the heart. The contribution is small at short lengths but increases greatly at lengths longer than about 2.10 μm. This conclusion is in agreement with the work reported by Brady (1991b) and by MacKenna et al. (1994) in which passive pressure-volume curves of the left ventricle were measured, and in which it was shown that the passive pressure was reduced after the heart was perfused with collagenase. Our conclusion that collagen develops passive tension is different, however, from the one reached in a recent study (Linke et al., 1994) in which the passive tension produced by single myofibrils isolated from rabbit cardiac muscle were measured. By comparing their results with the passive tension-length curves obtained by others on rat trabeculae and rat papillary muscle, the authors concluded that over the working range of the heart, passive tension resides solely in the myofibrils. An explanation for the difference between the conclusion of Linke et al. (1994) and ours may be our finding that the contribution of collagen in rat trabeculae was permanently diminished after the preparation had been stretched to lengths longer than about 2.2 μm. In the experiments reported here, we therefore carefully avoided stretch beyond 2.2 μm, allowing us to obtain passive tension-length curves that were highly reproducible. Because the sarcomere length range used in the studies on trabeculae and papillary muscle cited by Linke et al. (1994) exceeded 2.2 μm, it is possible that the tension generating potential of collagen was damaged.

Furthermore, mechanical protocols used by Linke et al. (1994) were different from those of the work on trabeculae that they cite. The details of the protocols used for generating passive tension are important because they influence the amount of passive tension that will develop. For example, myocytes at a sarcomere length of 2.2 μm reproducibly develop about twice as much passive tension when they are stretched from 1.9 μm to this length than when they are released from 2.4 μm to this length (length change completed in ~7 s and tension measured 90 s after end of stretch, as in Linke et al., 1994; H. L. Granzier, unpublished observations). In our work, we therefore carefully standardized the protocols that were used to measure passive tension, and we prevented stretch of trabeculae beyond 2.2 μm, which allowed us to compare results from myocytes with those from trabeculae and to conclude that collagen indeed contributes to passive tension of rat trabeculae at physiological sarcomere lengths. It is also important to note that the degree to which collagen contributes to passive tension in different parts of the heart is not necessarily the same as reported here for trabeculae, because the distribution and size of collagen fibrils has been found to vary somewhat in different parts of the heart (Robinson et al., 1983).

Titin

Rat cardiac titin has a molecular mass of about 2.5 MDa, which is 0.3–0.5 MDa less than titin from vertebrate skeletal muscle (Table 1). The lower molecular mass of cardiac titin is likely to have important functional consequences. We can predict these from the ~2.5 MDa/μm linear mass of titin (Wang et al., 1991) and assuming that 0.8 μm of the contour length of titin is in the A-band (cf. Wang et al., 1991). Based on these values, rat cardiac titin will have a contour length of 0.99 μm, with an extensible titin segment in the I-band that is only 0.19 μm. This is much shorter than in mammalian skeletal muscle (Table 1); for example, in rabbit semitendinosus muscle the extensible titin segment is 0.37 μm. Because the strain of the extensible titin segment is the fundamental determinant of the amount of passive tension that will be developed (Wang et al., 1991, 1993; Granzier and Wang, 1993b), we can predict that the much shorter extensible titin segment should increase passive tension in cardiac muscle much more steeply as sarcomere length increases than is the case in skeletal muscle.

This is exactly what we found: titin-based passive tension of cardiac muscle rises much faster with sarcomere length than it does in skeletal muscle. This is indicated, for example, by its much higher exponent of exponential tension rise (13 vs. ~3) and the much higher initial elastic modulus E_0 (23 vs. ~6); see Table 2 and Granzier and Wang (1993b). The difference between cardiac and skeletal muscle is graphically depicted in Fig. 10 *A* where we superimposed the tension derived from rat cardiac titin with that from rabbit semitendinosus titin (from Granzier and Wang, 1993b), both measured with the same protocol (i.e., identical I-band strain rate). The tension difference is especially large at the physiological sarcomere lengths of the heart. For example, at a sarcomere length of 2.20 μm cardiac titin develops more than 20 times the tension of skeletal muscle titin (17 vs. 0.7 kN m^{-2}). Thus, despite the fact that cardiac muscle has at those lengths a quite capable extracellular passive tension generator, i.e., collagen, a good intracellular passive tension generator is apparently also needed, probably to fulfill functions that cannot be performed by collagen, such as keeping the A-band centered in the sarcomere during contraction.

Titin-based tension at long sarcomere lengths

The lower molecular mass of cardiac titin is also predicted to affect the titin-based passive tension at long sarcomere

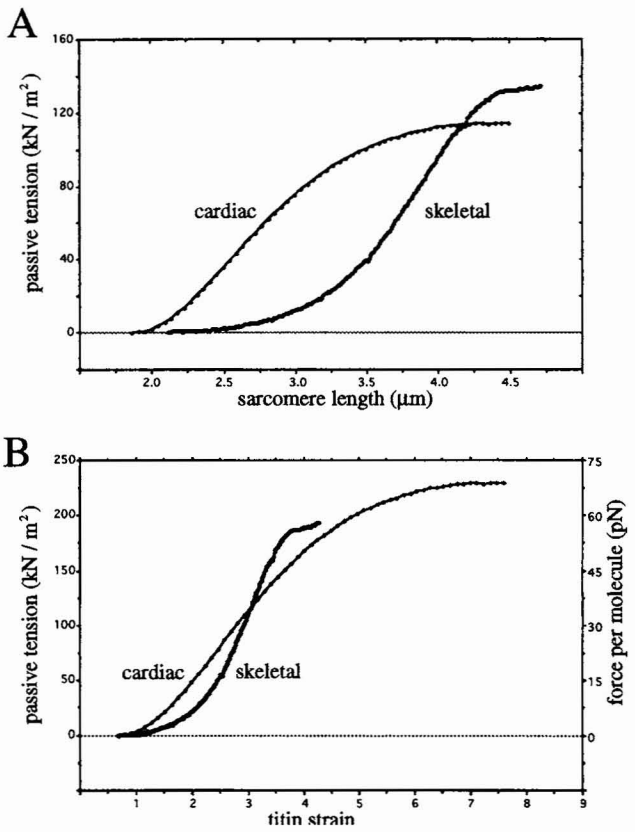

FIGURE 10 Comparison of titin-based passive tension from cardiac cells with that from skeletal muscle fibers. (*A*) Passive tension-sarcomere length relation. At short lengths, cardiac cells generate much more tension than skeletal muscle. Cross sectional area used to calculate tension includes both myofibrillar and nonmyofibrillar space. (*B*) Passive tension versus titin strain (left-hand scale) and force per titin molecule versus titin strain (right-hand scale). Strain calculated as explained in the text. Passive tension is per myofibrillar cross sectional area; force per titin molecule is determined as explained in the text. For cardiac muscle, the KCl/KI-sensitive tension of myocytes is used (same data as in Fig. 4 *A*), and for skeletal muscle data from rabbit semitendinosus muscle (same data as in Granzier and Wang, 1993b (their Fig. 12 *A*).

lengths. In various skeletal muscle types as well as in insect indirect flight muscle, it has been found that passive tension reaches a plateau at sarcomere lengths (defined as yield point) where the extensible segment of titin in the I-band is strained by a factor of about 3–4 (Wang et al., 1993; Granzier and Wang, 1993b). Using immunoelectron microscopy to study titin epitope behavior as a function of stretch, Wang et al. (1993) found evidence that the passive tension yield-point in skeletal muscle occurs when titin is forcibly detached from its anchor points in the A-band, thereby recruiting it to the extensible titin pool. It is also known that about 0.1–0.2 μm before the tension yield-point is reached, stiffness starts to decrease and continues to decrease at lengths where tension is at a plateau (Granzier and Wang, 1993b). In those studies, stiffness was measured with a constant amplitude sinusoid. As the length of the extensible titin segment increases, because of recruitment of A-band titin, the constant amplitude of the sinusoid decreases in proportion to the length of the extensible titin segment, and stiffness will go down accordingly. Stiffness decrease is thus a mechanical manifestation of recruitment of titin from the inextensible to the extensible pool.

We predict then that, if a yield point in cardiac muscle is found at an extensible titin strain similar to that in the other muscle types, the yield-point in rat cardiac muscle should occur at a sarcomere length of about 2.9 μm and stiffness should start to decrease at a sarcomere length of 2.7–2.8 μm.

In cardiac cells, a tension yield-point is indeed found (Fig. 4 *A*), but it occurs at a length of about 4.1 μm, which is 1.2 μm longer than where the yield-point is expected. In Results we showed that it is unlikely that the discrepancy between measurement and prediction is caused by sarcomere length inhomogeneity. An alternative explanation for the discrepancy is that recruitment of A-band titin in cardiac muscle occurs at an extensible titin strain that is much higher than in other muscle types. However, our stiffness results seem to argue against this. Stiffness was found to decrease from about 2.8 μm onwards (Fig. 4 *B*), as predicted based on the findings in skeletal muscle and allowing for the shorter extensible titin segment in cardiac muscle. Thus, it seems that recruitment does occur where predicted, but that passive tension continues to increase beyond this length because of some unknown mechanism.

Tension also responds differently than expected when titin is recruited from the thick filaments by extracting myosin with KCl (Fig. 6). For example, after a 60-min extraction, the thick filament length decreases about 60%, which adds a segment of 0.5-μm titin from the A-band to the extensible titin pool, increasing its unstrained length from 0.2 to 0.7 μm. Tension in Fig. 6 was measured at a sarcomere length of 2.7 μm, and it can be calculated that the strain of the extensible titin segment before extraction was ~3, and after extraction only ~0.7. This decrease in strain is predicted to result in zero tension (Fig. 10 *B*), whereas the measured tension is still as much as 60% of the control value. Tension is thus higher than predicted after recruitment caused by depolymerizing thick filaments, just as it is after recruitment caused by stretching sarcomeres beyond the yield-point. More experiments are needed to explain this finding. Immunolabeling of titin epitopes and studying their elastic behavior after recruitment to the extensible titin pool may be a useful way to proceed.

Force per titin molecule

An important conclusion of our work is that at sarcomere lengths that correspond to the working range of the heart, titin develops much higher tensions in cardiac muscle than in skeletal muscle. As was indicated above, the much shorter extensible titin segment of cardiac muscle is likely to underlie at least part of this difference. In addition, cardiac titin may also have different intrinsic properties and develop higher forces for a given strain than skeletal muscle titin does. This possibility was addressed by converting the measured passive tensions into force per titin molecule, and by comparing the results obtained from rat cardiac myocytes

with those from skeletal muscle. For comparison, we used the measurements on rabbit semitendinosus muscle (Granzier and Wang, 1993b), both because they were made using stretch protocols that resulted in the same I-band strain rate as those imposed on cardiac myocytes and because this muscle expresses the largest titin isoform known (2.94 MDa), making it as different from cardiac muscle as possible.

The measured tensions from the two muscle types were first normalized to their myofibrillar cross sectional area, assuming that the myofibrils occupy ~50% of the total cross sectional area in cardiac muscle (Page, 1971; Eisenberg, 1983) and ~70% in rabbit semitendinosus (Eisenberg, 1983). Normalized tension was plotted versus the strain of the extensible titin segment, calculated by subtracting half of the A-band width from half the measured sarcomere length and dividing this by the length of the unstrained extensible titin segment (cf. Wang et al., 1991). The results from myocytes and skeletal muscle fibers so obtained are shown in Fig. 10 *B* (left-hand scale). The curves are remarkably similar, certainly compared with the large differences between passive tension of cardiac and skeletal muscle that exist at the sarcomere length level (Fig. 10 *A*).

We converted the passive tension normalized per myofibrillar cross sectional unit area into force developed per titin molecule, by first estimating the number of thick filaments per μm^2 myofibrillar area, using the inter-thick filament spacing (Sp) and the $d_{1,0}$ lattice spacing determined by x-ray diffraction of tissue that is skinned and at its slack length. The Sp and $d_{1,0}$ literature values for cardiac muscle (Matsubara and Milman, 1974; Matsubara, 1980) and rabbit skeletal muscle (Huxley, 1968; Rome, 1972; Haselgrove, 1983) are the same: Sp is 46 nm, and $d_{1,0}$ is 40 nm. Based on these values, we calculated that there are 540 thick filaments per μm^2 myofibril in both muscle types. The number of titin molecules per μm^2 can be estimated from the number of titin molecules per half thick filament. Various studies by others have shown that this number is likely to be 6 (Wang, 1985; Maruyama, 1986; Trinick, 1991). We obtained in this study numbers that were either slightly higher (cardiac) or slightly lower (semitendinosus) than 6 (Table 1), but the differences were not statistically significant, and we will assume, therefore, 6 titin filaments per half thick filament in both cardiac and skeletal muscle. The estimated force per titin molecule versus titin strain (Fig. 10 *B*, right-hand scale) shows only small differences between cardiac and skeletal muscle. Although we cannot rule out functional significance for these small differences, overall these relationships are remarkably similar.

In conclusion, because rat cardiac muscle expresses a titin isoform of low molecular mass, the extensible I-segment of titin is much shorter in this muscle type than in skeletal muscle. Therefore, the extensible titin segment will be strained to a higher degree for a given sarcomere stretch, and this appears to be the main reason why cardiac titin is able to develop higher tensions at short sarcomere lengths. By expressing titin of various lengths, without changing the properties of titin itself, muscle has a straightforward means of manipulating passive tension.

Microtubules

In adult cardiac myocytes, microtubules are found around the myofibrils and in areas close to the mitochondria, plasma membrane, and nuclear membranes (for review, see Rappaport and Samuel, 1988). Microtubules have been implicated to mechanically obstruct sarcomere shortening in the activated hypertrophied myocardium (Tsutsui et al., 1993, 1994). We investigated whether microtubules contribute to the mechanical properties of passive cardiac cells upon stretch. Results varied from cell to cell (Fig. 7 *A*). Some cells show upon the addition of colchicine a clear drop in both tension and stiffness, whereas other cells do not respond at all. This variation may be related to the considerable variation in the microtubular network that exists in different myocytes of the adult rat heart (Rappaport and Samuel, 1988). Cells that did respond to colchicine may have had a more extensive network of microtubules than those that did not. In those cells that respond to colchicine, the microtubular-based passive tensions may very well serve important functions, for example, they might be part of a signal transduction pathway. However, on average (Fig. 7 *B*) microtubules do not seem to be important in determining the longitudinal passive properties of cardiac cells.

Intermediate filaments

Our results indicate that intermediate filaments contribute to passive tension of cardiac cells, even at the slack length (Fig. 4 *A*). Intermediate filaments in cardiac cells consist mainly of the protein desmin, which forms filaments of 10–12 nm width that make up a transversely oriented network that surrounds myofibrils at the level of the Z-band, and a longitudinal network present in the intermyofibrillar spaces (Tokuyasu, 1983). It is likely that this longitudinal network is responsible for the intermediate filament-based passive tension that we found.

In skeletal muscle fibers, intermediate filaments have also been reported to develop passive tension (Wang et al., 1991, 1993; Granzier and Wang, 1993b), but only at lengths longer than ~4–5 μm and at levels severalfold less then what we found in this study for cardiac cells. It is possible that these lower tensions in skeletal muscle fibers are a result of the fact that fibers had been mechanically skinned, which is likely to remove some intermediate filaments from the periphery of the fiber, whereas we used chemically skinned myocytes for our study. The difference between cardiac and skeletal muscle may also be explained by the finding of Price (1984) that cardiac muscle contains more than 5 times as much desmin as skeletal muscle, which is expected to increase the total cross sectional area of the intermediate filament system. It is interesting that when the intermediate filament tension of cardiac cells is scaled down by a factor five, tensions at

lengths >4.5 μm are similar to those of skeletal muscle (H. L. Granzier, unpublished observations). It seems likely, therefore, that the difference between the intermediate filament based passive tension of cardiac muscle and skeletal muscle is mainly due to the much higher content of desmin in cardiac muscle.

It has been proposed that the longitudinally oriented intermediate filaments in skeletal muscle function as a safety device that prevents damaged sarcomeres from being stretched during activation, by undamaged sarcomeres in series, to extreme lengths where they would be torn apart (Wang et al., 1993). In cardiac muscle, intermediate filaments may serve a similar function. The fact that the intermediate filament system in cardiac muscle is functional at shorter sarcomere lengths and develops higher tensions would then suggest that cardiac muscle is more sensitive to sarcomere damage due to overstretch and needs a higher degree of protection.

This work is an outgrowth of work done by Professor Allan Brady and Henk Granzier in the laboratory of Professor Kuan Wang at the University of Texas at Austin (Henk Granzier was supported by NIH grant DK20270 to Kuan Wang). We appreciate their continued support and encouragement. We express our gratitude to Bronislava Stockman for superb technical assistance and to Mitchell Luce for dissecting the rat trabeculae. This work was supported by a Grant-in-Aid from the American Heart Association (Washington State Affiliate) and a grant from the Whitaker Foundation.

REFERENCES

Allen, D., and J. Kentish. 1985. The cellular basis of the length-tension relation in cardiac muscle. *J. Mol. Cell. Cardiol.* 17:821–840.

Bihler, T., K. Ho, and P. Sawh. 1983. Isolation of Ca^{2+}-tolerant cells from adult rat heart. *Can. J. Physiol. Pharmacol.* 62:581–588.

Brady, A. 1991a. Cardiac myocyte mechanics. *Physiol. Rev.* 71:413–424.

Brady, A. 1991b. Length dependence of passive stiffness in single cardiac myocytes. *Am. J. Physiol.* 260:H1062–H1071.

Brady, A., and S. Farnsworth. 1986. Cardiac myocyte stiffness following extraction with detergent and high salt solutions. *Am. J. Physiol.* 250: H932–H943.

de Tombe, P., and H. ter Keurs. 1992. An internal viscous element limits unloaded velocity of sarcomere shortening in rat myocardium. *J. Physiol.* 454:619–642.

Eisenberg, B. 1983. Quantitative ultrastructure of mammalian skeletal muscle. *In* Handbook of Physiology, Skeletal Muscle. American Physiological Society, Bethesda, MD. 73–113.

Fabiato, A. 1988. Computer programs for calculating total from specific free or free from specific total ionic concentrations in aqueous solutions containing multiple metals and ligands. *Methods Enzymol.* 157:378–417.

Funatsu, T., T. H. Higuchi, and S. Ishiwata. 1990. Elastic filaments in skeletal muscle revealed by selective removal of thin filaments with plasma gelsolin. *J. Cell Biol.* 110:53–62.

Furst, D., M. Osborn, M. Nave, and K. Weber. 1988. The organization of titin filaments in the half-sarcomere revealed by monoclonal antibodies in immunoelectron microscopy: a map of ten nonrepetitive epitopes starting at the Z-line extends close to the M-line. *J. Cell Biol.* 106:1563–1572.

Granzier, H. L. M., J. Myers, and G. H. Pollack. 1987. Stepwise shortening of muscle fiber segments. *J. Muscle Res. Cell Motil.* 8:242–251.

Granzier, H. L. M., and G. H. Pollack. 1990. The descending limb of the force-sarcomere length relation revisited. *J. Physiol.* 421:595–617.

Granzier, H. L. M., H. E. D. J. ter Keurs, and H. A. Akster. 1991. Effect of thin filament length on the force-sarcomere length relation of skeletal muscle. *Am. J. Physiol.* C1060–C1070.

Granzier, H. L. M., and K. Wang. 1993a. Interplay between passive tension and strong and weak cross-bridges in insect asynchronous flight muscle: a functional dissection by gelsolin mediated thin filament removal. *J. Gen. Physiol.* 101:235–270.

Granzier, H. L. M., and K. Wang. 1993b. Passive tension and stiffness of vertebrate skeletal muscle and insect flight muscle: the contribution of weak crossbridges and elastic filaments. *Biophys. J.* 65: 2141–2159.

Granzier, H. L. M., and K. Wang. 1993c. Gel electrophoresis of giant proteins: solubilization and silver staining of titin and nebulin from single muscle fiber segments. *Electrophoresis.* 14:56–64.

Haselgrove, J. 1983. Structure of vertebrate striated muscles as determined by x-ray-diffraction studies. *In* Handbook of Physiology, Skeletal Muscle. American Physiological Society, Bethesda, MD. 143–173.

Huxley, H. E. 1968. Structural difference between resting and rigor muscle: evidence from the intensity changes in the low-angle equatorial x-ray diagram. *J. Mol. Biol.* 37:507–520.

Huxley, A. F., and R. Niedergerke. 1958. Measurements of the striations of isolated muscle fibres with the interference microscope. *J. Physiol.* 144: 403–425.

Higuchi, H. 1992. Changes in contractile properties with selective digestion of connectin (titin) in skinned fibers of frog skeletal muscle. *J. Biochem.* 111:291–295.

Higuchi, H., T. Suzuli, S. Kimura, S. Yoshioka, K. Maruyama, and Y. Umazuma. 1992. Localization and elasticity of connectin filaments in skinned frog muscle fibers subjected to partial depolymerization of thick filaments. *J. Muscle Res. Cell Motil.* 13:285–294.

Hofman, P. A., H. Hartzell, and R. Moss. 1991. Alterations in Ca sensitive tension due to partial extraction of C-protein from rat skinned cardiac myocytes and rabbit skeletal muscle fibers. *J. Gen. Physiol.* 97:1141–1163.

Horowits, R., E. S. Kempner, M. E. Bisher, and R. Podolsky. 1986. A physiological role for titin and nebulin in skeletal muscle. *Nature.* 323: 160–164.

Horowits, R., and R. Podolsky. 1987. The positional stability of thick filaments in activated skeletal muscle: evidence for the role of titin filaments. *J. Cell Biol.* 105:2217–2223.

Kitazawa, T., S. Kobayashi, K. Horiuto, A. Somlyo, and A. Somlyo. 1989. Receptor-coupled, permeabilized smooth muscle. *J. Biol. Chem.* 264: 5339–5342.

Krueger, J. W., and K. Tsujioka. 1986. Sarcomere mechanics towards a physical basis for cardiac contraction. *In* Some Mathematical Questions in Biology-Muscle Physiology, Vol. 16. R. M. Miura, editor. American Mathematical Society, Providence, RI. 122–155.

Kruger, M., J. Wright, and K. Wang. 1991. Nebulin as a length regulator of thin filaments of vertebrate skeletal muscles: correlation of thin filament length, nebulin size, and epitope profile. *J. Cell Biol.* 115:97–107.

Labeit, S., M. Gautel, A. Lackey, and J. Trinick. 1992. Towards a molecular understanding of titin. *EMBO J.* 11:1711–1716.

Labeit, S., D. Barlow, M. Gautel, T. Gibson, J. Holt, C. Hsieh, U. Francke, K. Leonard, J. Wardale, A. Whiting, and J. Trinick. 1990. A regular pattern of two types of 100-residue motif in the sequence of titin. *Nature.* 345:273–276.

Linke, W., V. Popov, and G. Pollack. 1994. Passive and active tension in single cardiac myofibrils. *Biophys. J.* 67:782–792.

MacKenna, D., J. Omens, A. McCulloch, and J. Covell. 1994. Contribution of collagen matrix to passive left ventricular mechanics in isolated rat hearts. *Am. J. Physiol.* 266:H1007–H1018.

Maruyama, K. 1986. Connectin an elastic filamentous protein of striated muscle. *Int. Rev. Cytol.* 104:81–114.

Maruyama, K., S. Kimura, M. Juroda, and S. Handa. 1977. Connectin (titin), an elastic protein of muscle. Its abundance in cardiac muscle. *J. Biochem.* 82:347–350.

Matsubara, I. 1980. X-ray diffraction studies of the heart. *Annu. Rev. Biophys. Bioeng.* 9:81–105.

Matsubara, I., and B. Millman. 1974. X-ray diffraction patterns from mammalian heart muscle. *J. Mol. Biol.* 82:527–536.

Morano, I., K. Hadlicke, S. Grom, A. Koch, H. Schwinger, M. Bohm, S. Bartel, E. Erdmann, and E. Krause. 1994. Titin, myosin light chains and C-protein in the developing and failing human heart. *J. Mol. Cell. Cardiol.* 26:361–368.

Page, S., L. McCallister, and B. Power. 1971. Stereological measurements of cardiac ultrastructures implicated in excitation-contraction coupling. *Proc. Natl. Acad. Sci. USA.* 68:1464–1466.

Price, M., 1984. Molecular analysis of intermediate filament cytoskeleton—a putative load bearing structure. *Am. J. Physiol.* 246: H566–H572.

Rappoport, L., and J. Samuel. 1988. Microtubules in cardiac myocytes. *Int. Rev. Cytol.* 113:101–143.

Robinson, T., L. Cohen-Gould, and S. Factor. 1983. Skeletal framework of mammalian heart muscle. Arrangement of inter- and pericellular connective tissue structures. *Lab. Invest.* 49:482–498.

Robson, R., and T. Huiatt. 1983. Roles of the cytoskeletal proteins desmin, titin and nebulin in muscle. *Reciprocal Meat Conf. Proc.* 36:116–124.

Rodriguez, E., W. Hunter, M. Royce, M. Leppo, A. Douglas, and H. Weisman. 1992. A method to reconstruct myocardial sarcomere lengths and orientations at transmural sites in beating canine hearts. *Am. J. Physiol.* 263:H293-H306.

Rome, E. 1972. Relaxation of glycerinated muscles: low-angle x-ray diffraction studies. *J. Mol. Biol.* 65:331–345.

Roos, K., and A. Brady. 1989. Stiffness and shortening changes in myofilament-extracted rat cardiac myocytes. *Am. J. Physiol.* 256: H539–H551.

Samuel, J., K. Schwartz, A. Lompre, C. Delcayre, F. Marotte, B. Swynghedauw, and L. Rappaport. 1983. Immunological quantitation and localization of tubulin in adult rat heart isolated myocytes. *Eur. J. Cell Biol.* 31:99–106.

Schliwa, M., J. Blerkom, and K. Porter. 1981. Stabilization of the cytoplasmic ground substance in detergent-opened cells and a structural and biochemical analysis of its composition. *Proc. Natl. Acad. Sci. USA.* 78:4329–4333.

Slayter, E. M., and H. S. Slayter. 1992. Light and Electron Microscopy. Cambridge University Press, Cambridge.

Squire, J. 1986. Muscle: Design, Diversity and Disease. The Benjamin/Cummings Publishing Company, Menlo Park, CA.

Sweitzer, N., and R. Moss. 1993. Determinants of loaded shortening velocity in single cardiac myocytes permeabilized with α-hemolysin. *Circ. Res.* 73:1150–1162.

Sten-Knudsen, O. 1953. Torsional elasticity of the isolated cross-striated muscle fibre. *Acta Physiol. Scand.* 28:1–240.

Tokuyasu, K. 1983. Visualization of longitudinally-oriented intermediate filaments in frozen sections of chicken cardiac muscle by a new staining method. *J. Cell Biol.* 97:562–565.

Trinick, J. 1991. Elastic filaments and giant proteins in muscle. *Curr. Opin. Cell Biol.* 3:112–118.

Tsutsui, H., K. Ishihara, and G. Cooper. 1993. Cytoskeletal role in the contractile dysfunction of hypertrophied myocardium. *Science.* 260:682–687.

Tsutsui, H., H. Tagawa, R. Kent, P. McCollam, K. Ishihara, M. Nagatsu, and G. Cooper. 1994. Role of microtubules in contractile dysfunction of hypertrophied cardiocytes. *Circulation.* 90:533–555.

Wang, K. 1985. Sarcomere-associated cytoskeletal lattices in striated muscle. *Cell Muscle Motil.* 6:315–369.

Wang, K., R. McCarter, J. Wright, B. Jennate, and R. Ramirez-Mitchell. 1991. Regulation of skeletal muscle stiffness and elasticity by titin isoforms: a test of the segmental extension model of resting tension. *Proc. Natl. Acad. Sci. USA.* 88:7101–7109.

Wang, K., R. McCarter, J. Wright, B. Jennate, and R. Ramirez-Mitchell. 1993. Viscoelasticity of the sarcomere matrix of skeletal muscles: the titin-myosin composite filament is a dual-range molecular spring. *Biophys. J.* 64:1161–1177.

Wang, K., and R. Ramirez-Mitchell. 1983. A network of transverse and longitudinal intermediate filaments is associated with sarcomeres of adult vertebrate skeletal muscle. *J. Cell Biol.* 96:562–570.

Wang, K., J. Wright, and R. Ramirez-Mitchell. 1984. Architecture of the titin/nebulin containing cytoskeletal lattice of the striated muscle sarcomere—evidence of elastic and inelastic domains of the bipolar filaments. *J. Cell Biol.* 99:435*a*. (Abstr.)

Weber, K., Y. Sun, S. Tyagi, and J. Cleutjens. 1994. Collagen network of the myocardium: function, structural remodelling and regulatory mechanisms. *J. Mol. Cardiol.* 26:279–292.

Yoshioka, T., H. Higuchi, S. Kimura, K. Ohashi, Y. Umazume, and K. Maruyama. 1986. Effects of mild trypsin treatment on the passive tension generation and connectin splitting in stretched skinned fibers from frog skeletal muscle. *Biomed. Res.* 7:181–186.